isvr Institute of Sound and Vibration Research

Structural Analysis of a Combined Beam and Plate Structure using a Wave Approach

J. Woo Yoo, N.S. Ferguson and D.J. Thompson

ISVR Technical Memorandum No 888

June 2002

University of Southampton

SCIENTIFIC PUBLICATIONS BY THE ISVR

Technical Reports are published to promote timely dissemination of research results by ISVR personnel. This medium permits more detailed presentation than is usually acceptable for scientific journals. Responsibility for both the content and any opinions expressed rests entirely with the author(s).

Technical Memoranda are produced to enable the early or preliminary release of information by ISVR personnel where such release is deemed to the appropriate. Information contained in these memoranda may be incomplete, or form part of a continuing programme; this should be borne in mind when using or quoting from these documents.

Contract Reports are produced to record the results of scientific work carried out for sponsors, under contract. The ISVR treats these reports as confidential to sponsors and does not make them available for general circulation. Individual sponsors may, however, authorize subsequent release of the material.

UNIVERSITY OF SOUTHAMPTON

INSTITUTE OF SOUND AND VIBRATION RESEARCH

DYNAMICS GROUP

Structural Analysis of a Combined Beam and Plate Structure using a Wave Approach

by

Ji Woo Yoo, N.S. Ferguson and D.J. Thompson

ISVR Technical Memorandum No: 888

June 2002

Contents

1. Introduction

Even though the dynamic characteristics of most simple structures such as a beam or plate can be solved theoretically, there are a lot of difficulties in obtaining solutions for combinations of such structures. As such combined structures form the basis of practical industrial structures, much attention has been focused on getting exact solutions or approximate results.

Low frequency analysis has been traditionally important because it represents the fundamental characteristics of a structure and some useful and powerful numerical methods have been developed for this analysis range. The most common of these is the finite element method. In this method, a structure is represented by a number of elements and the accuracy of the result can usually be improved by increasing the number of elements. It is known that, in general, more than four elements are needed per half wavelength [1] and this means that for more accurate results in the higher frequency range, a large number of elements should be included.

Although the upper frequency limit can be extended owing to the rapid development of computer hardware, the need for large computer resources as well as inherent problems at high frequencies remain as obstacles to its implementation [2]. In particular there are considerable uncertainties in modelling actual structures at high frequencies and the details of the response are sensitive to small changes in this frequency range.

The Statistical Energy Analysis method, SEA, is a good alternative for high frequency analysis. In SEA, it is assumed that the response is diffuse within each subsystem, so that only the total vibrational energy in each subsystem is important. The energy transfer between subsystems is determined by the coupling loss factor [3]. Because each subsystem or substructure corresponds to only one element of the solution matrix, it is a relatively simple, efficient and low cost method. But in practical application, there are some difficulties. One of them is to find the

relevant coupling loss factors. To ensure more accurate results for practical structures, more diverse coupling loss factors for the corresponding structures should be defined [4]. Ideally for the application of SEA the subsystems or substructures should be weakly coupled. In addition, for any particular frequency band each substructure should contain a minimum number of modes whose natural frequency falls within the band and there should ideally be equi-partition of vibrational energy between the modes of a substructure [5]. Because of these assumptions, the accuracy of the predicted average energy is limited and it seems to be impractical to analyse a system containing components carrying a long wavelength or having a low modal density. This results in a low frequency limit of applicability.

There has been much effort to overcome the limitations mentioned above and to find suitable methods for the region between these two frequency ranges, known as the mid-frequency region. Various alternative methods, energy flow methods [6-9], wave approaches [10-13], fuzzy structure theory [14, 15], and a hybrid method [16] have been presented.

Wohlever and Bernhard [6] have studied an energy flow method in one-dimensional systems. On the assumptions that a structure has light damping and that the kinetic energy density and potential energy density are equal, a second order differential equation governing the energy distribution was developed and applied to coupled rod or coupled beam systems. Also Bouthier and Berhnard [7] applied this equation to membranes where the response can be reasonably described in terms of plane waves. In this research, to get an approximate energy distribution, an equation for the time-averaged energy density was used with a smoothing operation which means a space-averaging procedure over the span of the trace wavelength. The accuracy of this method is improved as the frequency of excitation and the damping increase, but at low frequency the approximations are not suitable because there are not enough modes in the frequency band of interest.

Another energy flow method was developed for a jointed beam structure by Shankar and Keane [8,9]. Under the some limiting conditions, for example, the beams are not allowed to be coupled at the mid-span and the boundary conditions are only hinged or clamped conditions, the averaged energy levels were studied using the receptances at the grid of joints between beams. The behaviour of the global structure made of rigidly jointed beams is predicted from Green s functions of the individual uncoupled beams. This approach has some advantages, for example, local damping can be used for the corresponding substructure and the finite element method can be used. However, difficulties in the convergence of the Green's function can require the inclusion of a large number of modes.

A wave approach based on the reflection and transmission of a wave along a structure and at its joints has been studied for the prediction of the frequency response. Hugin [10] described the response and transmitted power of bending waves in structures consisting of beams on the assumption that the influence of the near fields is negligible. Grice and Pinnington [11,12] used a wave analysis to study a built-up structure consisting of a beam and plate using the assumption that short waves in a flexible plate present a locally reacting impedance to the long waves at the structural joints [13]. In general, this method is useful for the simple structure combination considered but a more general approach is required to deal with practical structures.

For the analysis of the mid-frequency range, Soize [14] introduced fuzzy structure theory. A fuzzy structure is defined as the set of uncertain substructures which are attached to a master structure but are not accessible by classical modelling and are therefore modelled by probabilistic concepts. Strasberg and Feit [15] derived a more simple expression for the vibration damping induced by a multitude of small sprung masses without using a probabilistic approach and applied this to a simple structure consisting of a beam and a plate. From these studies, it is known that the fuzzy structure behaves mainly as damping to the master structure and the level of the

damping is independent of the dissipation factor of the attachments. In practice, because a structure is divided into a master structure and a fuzzy structure, application is limited to relatively simple structures or structures with a clear division between master and fuzzy components.

The methods described above have both advantages and disadvantages. Comparing these methods, it seems that using a combined or hybrid method is a reasonable approach. This is because, to overcome the disadvantage of the finite element method in the high frequency range, it is necessary to use a form of average method. Conversely, in the low modal density region, it is inevitable that a deterministic method such as the finite element method should be used.

One such hybrid method was developed by Langley and Bremner [16]. In this method, the degrees of freedom of a system are partitioned into a global set and a local set. For the analysis of a simple rod system, global equations of motion are formulated in a deterministic manner and local equations of motion are solved by statistical energy analysis.

The present project is related to the development of a practical hybrid method and the aim of this report is to understand the fundamental dynamic characteristics of a simple combined stucture which consists of a beam and a plate and, as the first step of the project, to study a method for combining simple structures using a wave approach.

The initial models considered are connected beams and plates. The beams possess low modal densities, and corresponding small wavenumbers, whilst the plate elements possess high modal densities and corresponding large wavenumbers. A model of a plate with a beam connected along one edge is considered. This is similar to the plate-stiffened beam considered by Grice and Pinnington [11, 12] except that the plate is only connected on one side of the beam in the present case.

2. Infinite beam coupled to semi-infinite plate

2.1 Undamped free wave motion

Consider a built-up structure or combined structure, in which a stiffer component carries long-wavelength flexural waves and a flexible component carries short-wavelength flexural waves. It is assumed that the ratio of these wavelengths is sufficiently large. It is known that the built-up structure can be analysed in terms of its dispersion relation. This report is concerned with this relationship for a simple built-up structure and the power transfer relationship in the built-up structure is presented.

Basically the analysis follows the derivation given by Grice and Pinnington [11, 12]. The case considered here is that of an infinite beam attached along the edge ($y = 0$) of a semi-infinite plate, see Figure 1. This differs from the case considered by Grice *et al* in which a beam was connected onto the middle of an infinite plate.

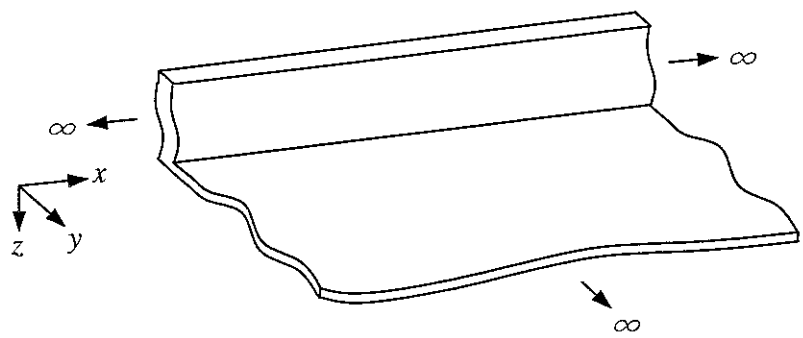

Figure 1. A built-up structure consisting of an infinite beam attached to a semi-infinite plate.

Consider first the uncoupled free wave motion of the beam and plate. The relevant equation of motion of the beam with no damping at frequency ω is

$$D_b \frac{\partial^4 \tilde{w}_b}{\partial x^4} - m_b' \omega^2 \tilde{w}_b = 0 \qquad (2.1)$$

where $\tilde{w}_b$ is the complex amplitude of the beam vibration, D_b is the bending stiffness given by EI with E Young's modulus and I the second moment of area and m_b' is the mass per unit length.

A propagating harmonic flexural wave in the infinite beam, uncoupled from the plate, is given by

$$\tilde{w}_b = \tilde{A} e^{-ik_b x} \qquad (2.2)$$

where $\tilde{A}$ is the wave amplitude, x is the coordinate in the direction of propagation and k_b is the uncoupled beam wavenumber given by $k_b^4 = (m_b'/D_b)\omega^2$. A time dependence of $e^{i\omega t}$ is assumed.

The equation of motion of the plate with no damping is

$$D_p \nabla^4 \tilde{w}_p - m_p'' \omega^2 \tilde{w}_p = 0, \quad \nabla^4 = \frac{\partial^4}{\partial x^4} + 2\frac{\partial^4}{\partial x^2 \partial y^2} + \frac{\partial^4}{\partial y^4} \qquad (2.3)$$

where D_p is the plate bending stiffness given by $D_p = \frac{Eh^3}{12(1-\nu^2)}$ and m_p'' is the mass per unit area of the plate. This leads to free wave solutions with wavenumber $k_p^4 = m_p'' \omega^2 / D_p$.

When the infinite plate and the infinite beam are joined along the line $y = 0$ a force per unit length $\tilde{F}(x)$ acts between them. Thus equation (2.1) becomes

$$D_b \frac{\partial^4 \tilde{w}_b}{\partial x^4} - m_b' \omega^2 \tilde{w}_b = -\tilde{F}(x) \tag{2.4}$$

Suppose that the free wave motion of the beam becomes

$$\tilde{w}_b = \tilde{A} e^{-ik_x x}. \tag{2.5}$$

Then by wavenumber trace matching the motion of the plate is given by

$$\tilde{w}_P = (\tilde{B} e^{-ik_y y} + \tilde{C} e^{-k_e y}) e^{-ik_x x} \tag{2.6}$$

where $\tilde{B}$ is the amplitude of the wave propagating away from the junction, $\tilde{C}$ is the amplitude of the near field wave in the plate which is also generated at the junction, k_x is the wavenumber in the coupled beam, k_y is the trace wavenumber for the propagating wave radiating into the plate normal to the beam and k_e is the trace wavenumber for the nearfield wave in the plate. In the above it is assumed k_x is real, although as will be seen this is not quite the case.

To obtain the propagating wavenumber k_x in terms of the beam and plate properties, consider the propagating wave solution in the plate $\tilde{w}_p = \tilde{B} e^{-ik_y y} e^{-ik_x x}$. Substituting this into equation (2.3) gives

$$D_p \{(k_x^4 + 2k_y^2 k_x^2 + k_y^4) - m_p'' \omega^2\} \tilde{B} e^{-ik_y y} e^{-ik_x x} = 0. \tag{2.7}$$

As $\tilde{B} e^{-ik_y y} e^{-ik_x x} \neq 0$, then $k_x^4 + 2k_y^2 k_x^2 + k_y^4 - k_p^4 = 0$ where $k_p^4 = m_p'' \omega^2 / D_p$ is the uncoupled plate wavenumber.

Therefore, the propagating trace wavenumber in the plate is found to be

$$k_y = \sqrt{k_p^2 - k_x^2}. \tag{2.8,a}$$

Similarly, let $\tilde{w}_p = \tilde{C}e^{-k_e y}e^{-ik_x x}$, then the near field wavenumber is

$$k_e = \sqrt{k_p^2 + k_x^2}\,. \tag{2.8,b}$$

The boundary conditions when a semi-infinite plate is attached at its edge to the beam are:

① Continuity equation; equal displacement

$$\tilde{w}_b(x) = \tilde{w}_p(x,0) \tag{2.9}$$

② Moment equilibrium condition*; it is assumed that no bending moment acts on the plate by the beam along $y=0$

$$D_p\left(\frac{\partial^2 \tilde{w}_p}{\partial y^2} + \nu\frac{\partial^2 \tilde{w}_p}{\partial x^2}\right)\Bigg|_{y=0} = 0 \tag{2.10}$$

③ Force equilibrium condition; the force on the plate is equal and opposite to the force on the beam

$$D_p\frac{\partial}{\partial y}\left(\frac{\partial^2 \tilde{w}_p}{\partial y^2} + (2-\nu)\frac{\partial^2 \tilde{w}_p}{\partial x^2}\right)\Bigg|_{y=0} = \tilde{F}(x)\,. \tag{2.11}$$

From the boundary condition ①,

$$\tilde{A} = \tilde{B} + \tilde{C}\,. \tag{2.12}$$

---

* Here it is assumed that the beam has no torsional stiffness. If the beam is assumed infinitely stiff to torsion the condition will become $\frac{\partial \tilde{w}_p}{\partial y} = 0$.

From the boundary condition ②,

$$D_p e^{-ik_x x}\left[-k_y^2\tilde{B}e^{-ik_y y}+k_e^2\tilde{C}e^{-k_e y}-\nu\left(k_x^2\tilde{B}e^{-ik_y y}+k_x^2\tilde{C}e^{-k_e y}\right)\right]_{y=0}=0. \qquad (2.13)$$

$$\tilde{C}=\frac{k_y^2+\nu k_x^2}{k_e^2-\nu k_x^2}\tilde{B}.$$

$$\tilde{A}=\tilde{B}+\tilde{C}=\frac{k_e^2-\nu k_x^2}{k_e^2-\nu k_x^2}\tilde{B}+\frac{k_y^2+\nu k_x^2}{k_e^2-\nu k_x^2}\tilde{B}=\frac{k_y^2+k_e^2}{k_e^2-\nu k_x^2}\tilde{B}.$$

Therefore, the amplitudes of the waves in the plate are given by

$$\tilde{B}=\frac{k_e^2-\nu k_x^2}{k_y^2+k_e^2}\tilde{A},\quad \tilde{C}=\frac{k_y^2+\nu k_x^2}{k_y^2+k_e^2}\tilde{A}. \qquad (2.14)$$

From the boundary condition ③,

$$\begin{aligned}
&D_p e^{-ik_x x}\frac{\partial}{\partial y}\left(-k_y^2\tilde{B}e^{-ik_y y}+k_e^2\tilde{C}e^{-k_e y}-(2-\nu)k_x^2\tilde{B}e^{-ik_y y}-(2-\nu)k_x^2\tilde{C}e^{-k_e y}\right)\Big|_{y=0}\\
&=D_p e^{-ik_x x}\left[ik_y^3\tilde{B}e^{-ik_y y}-k_e^3\tilde{C}e^{-k_e y}+i(2-\nu)k_x^2k_y\tilde{B}e^{-ik_y y}+(2-\nu)k_x^2k_e\tilde{C}e^{-k_e y}\right]_{y=0}\\
&=D_p e^{-ik_x x}\left[ik_y^3\tilde{B}-k_e^3\tilde{C}+i(2-\nu)k_x^2k_y\tilde{B}+(2-\nu)k_x^2k_e\tilde{C}\right]=\tilde{F}(x).
\end{aligned}$$

Substituting for $\tilde{B}$ and $\tilde{C}$ in terms of $\tilde{A}$ gives

$$\frac{-ik_y\left\{(2-\nu)k_x^2+k_y^2\right\}\left\{\nu k_x^2-k_e^2\right\}+k_e\left\{(2-\nu)k_x^2-k_e^2\right\}\left\{\nu k_x^2+k_y^2\right\}}{k_y^2+k_e^2}\tilde{A}D_p e^{-ik_x x}=\tilde{F}(x). \qquad (2.15)$$

Because $k_y^2 + k_x^2 = k_p^2, k_e^2 - k_x^2 = k_p^2$ and $k_y^2 + k_e^2 = 2k_p^2$, the numerator of the fraction in equation (2.15) becomes

$$ik_y\left\{(2-\nu)k_x^2 + k_p^2 - k_x^2\right\}\left\{\nu k_x^2 - k_p^2 - k_x^2\right\} + k_e\left\{(2-\nu)k_x^2 - k_p^2 - k_x^2\right\}\left\{\nu k_x^2 + k_p^2 - k_x^2\right\}$$
$$= ik_y\left\{(1-\nu)k_x^2 + k_p^2\right\}^2 - k_e\left\{(1-\nu)k_x^2 - k_p^2\right\}^2.$$

Therefore, equation (2.15) is equivalent to

$$\frac{i\sqrt{1-k_x^2/k_p^2}\left\{(1-\nu)k_x^2 + k_p^2\right\}^2 - \sqrt{1+k_x^2/k_p^2}\left\{(1-\nu)k_x^2 - k_p^2\right\}^2}{2k_p}\tilde{A}D_p e^{-ik_x x} = \tilde{F}(x), \tag{2.16}$$

and the line impedance of the plate, which is the impedance per unit length along the beam, is

$$\tilde{Z}_p' = \frac{\tilde{F}(x)}{i\omega\tilde{w}_p(x,0)} = \frac{\tilde{F}(x)}{i\omega\tilde{w}_b(x)},$$

$$\tilde{Z}_p' = \frac{D_p k_p^3\left[\sqrt{1-k_x^2/k_p^2}\left\{(1-\nu)k_x^2/k_p^2 + 1\right\}^2 + i\sqrt{1+k_x^2/k_p^2}\left\{(1-\nu)k_x^2/k_p^2 - 1\right\}^2\right]}{2\omega} \tag{2.17}$$

from which $\tilde{F}(x) = i\omega Z_p'\tilde{A}e^{-ik_x x}$. Note that equation (2.17) includes a damping-like term which is the real part of a complex number and also a mass-like imaginary term. These have an influence on the coupled beam which will be mentioned in section 2.5. Finally, the general dispersion relation for the infinite beam attached to the semi-infinite plate can be derived from equation (2.4), (2.16) and (2.17).

$$D_b k_x^4 = m_b'\omega^2 - i\omega\,\tilde{Z}_p'. \tag{2.18}$$

There are two propagating wave solutions and two evanescent wave solutions to this equation. It must be solved iteratively as k_x is contained in $\tilde{Z}'_p$. Note that k_x is not real, due to the damping-like term in $\tilde{Z}'_p$.

2.2 Forced response

Once the wavenumber for a built-up structure is calculated, then the point mobility of the structure can be easily calculated from the equation of the point mobility of an infinite beam. Although the point mobility of the infinite beam in flexure is well-known by Cremer *et al* [17] and given by

$$Y = \frac{\omega}{4D_b k_b^3}(1-i), \tag{2.19}$$

in the present report, a semi-infinite beam is considered in numerical analysis because it is more meaningful for comparing with a finite beam structure.

The point mobility of the semi-infinite beam in flexural motion can be derived from the general solution of the motion of a finite Euler-Bernoulli beam, which is given by

$$\tilde{w}(x) = \tilde{A}_1 e^{-ik_b x} + \tilde{A}_2 e^{-k_{nf} x} + \tilde{A}_3 e^{ik_b x} + \tilde{A}_4 e^{k_{nf} x}, \tag{2.20}$$

where $\tilde{A}_1$ and $\tilde{A}_3$ are the amplitudes of propagating waves, $\tilde{A}_2$ and $\tilde{A}_4$ are the amplitudes of the near field waves, the k_b is the propagating wavenumber and the k_{nf} is the near field wavenumber. Consider a semi-infinite beam located at $0 \le x \le \infty$, and excited at $x = 0$ by a force $\tilde{F}$ acting perpendicular to the beam axis. Since all waves propagate away from the excitation point, waves travelling in the negative direction x direction waves should vanish.

Therefore, $\tilde{A}_3 = \tilde{A}_4 \approx 0$, and equation (2.20) becomes

$$\tilde{w}(x) = \tilde{A}_1 e^{-ik_b x} + \tilde{A}_2 e^{-k_{nf} x}. \tag{2.21}$$

Because the applied moment is zero and the force applied should be the same as the shear force of the beam at $x = 0$, the boundary conditions are

$$D_b \left.\frac{\partial^2 w}{\partial x^2}\right|_{x=0} = 0, \quad -D_b \left.\frac{\partial^3 w}{\partial x^3}\right|_{x=0} = \tilde{F}. \tag{2.22 a, b}$$

Then the amplitudes $\tilde{A}_1$ and $\tilde{A}_2$ are calculated as follows.

$$\tilde{A}_1 = \frac{\tilde{F}}{D_b k_b^2 (-ik_b + k_{nf})}, \quad \tilde{A}_2 = \frac{\tilde{F}}{D_b k_{nf}^2 (-ik_b + k_{nf})}. \tag{2.23 a, b}$$

Therefore, the point mobility of the semi-infinite beam is

$$\tilde{Y}_0 = \left.\frac{i\omega \tilde{w}}{\tilde{F}}\right|_0 = \frac{i\omega}{D_b}\left[\frac{1}{k_b^2 (ik_b - k_{nf})} + \frac{1}{k_{nf}^2 (ik_b - k_{nf})}\right]. \tag{2.24}$$

Because $k_b = k_{nf}$ in an uncoupled semi-infinite beam, the point mobility becomes [17]

$$\tilde{Y}_0 = \frac{\omega}{D_b k_b^3}(1 - i). \tag{2.25}$$

The general relation of equation (2.18) is still valid for the built-up structure consisting of the semi-infinite beam shown in Figure 2 and the point mobility for the built-up structure can be calculated from equation (2.24) using the corresponding coupled propagating wavenumber k_x and the near field wavenumber k_{nf} of the built-up structure.

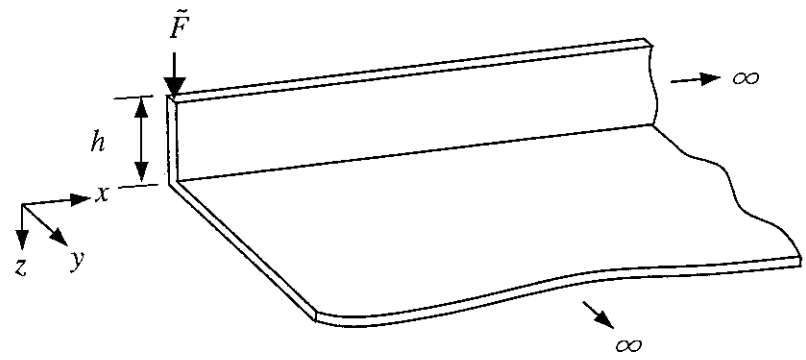

Figure 2. A built-up structure consisting of a semi-infinite beam attached to a semi-infinite plate.

2.3 Introduction of damping on the beam

The effect of damping in the beam can be introduced to the previous section by using $\tilde{D}_b$ which is given by D_b and the structural loss factor of the beam η_b as follows [17].

$$\tilde{D}_b = D_b(1+i\eta_b). \tag{2.26}$$

Provided η_b is small the above analysis remains approximately valid. However it should be realised that the derivation of k_y and k_e by wavenumber matching is strictly only applicable in the undamped case.

2.4 Approximation by locally reacting impedance

Note that if $k_p >> k_x$, i.e. the plate wavenumber is much larger than the wavenumber in the coupled beam, then the exact line impedance of the plate, equation (2.17) can be written approximately as

$$\tilde{Z}'_p\big|_{k_p>>k_x} \approx \frac{D_p k_p^3}{2\omega}(1+i) = \frac{m''_p \omega}{2k_p}(1+i). \qquad (2.27)$$

Equation (2.27) is known to be valid if the plate wavenumber is sufficiently larger than the coupled beam wavenumber, i.e., $k_x / k_p < 0.5$ [11]. Then the impedance of the plate can be considered as the input point impedance of an equivalent beam of infinite length and unit width driven by a point force (the inverse of equation (2.25)). Therefore, the plate is considered as locally reacting. This means that if the beam propagating wavelengths are much longer than those in the plate, then the wave radiates into the plate at an angle which is almost normal to the axis of the beam. From this point of view, the beam possessing the long waves is a 'spine' structure and the plate carrying short waves is the 'receiver'. If equation (2.27) is used, k_x^4 can be found directly from equation (2.18) from which the propagating wavenumber and the near field wavenumber in the beam can be calculated.

Strictly, the propagating wavenumber and the near field wavenumber could have different values, but in the present report, since wavenumber trace matching is only based on the propagating wave in the coupled beam, the exact near field wavenumber cannot be calculated. By assuming the locally reacting plate impedance, the near field wavenumber can be calculated approximately from the roots of k_x^4 in equation (2.18) without any assumption of trace matching.

2.5 Numerical analysis

Numerical analysis was performed for the structure shown in Figure 2. The material properties of the structure are shown in Table 1. The thicknesses of the beam and the plate are the

same and the area moment of inertia of the beam is calculated by assuming that its neutral axis lies in the mid-plane of the plate using

$$I_b = \frac{th^3}{12} + \frac{th(t+h)^2}{4} \tag{2.28}$$

where h is the beam height excluding the thickness of the plate and t is the thickness of the plate. The excitation point was selected at one end of the beam, $x = 0$, throughout the present report.

Table 1. Material properties and dimensions of the built-up structure consisting of a semi-infinite beam attached to a semi-infinite plate as in Figure 2.

Material	Perspex
Young's modulus, E (GN/m^2)	4.4
Poisson's ratio, ν	0.38
Density, ρ (kg/m^3)	1152.0
Thickness, t (mm)	5.9
Height of the beam, h (mm)	68.0
Loss factor of the beam (if used), η_b	0.05

As described in section 2.4, if the impedance of a plate can be regarded as locally reacting, the numerical analysis to identify the characteristics of a full structure will be greatly simplified.

Before using the simplification, it is necessary to verify that the assumption is applicable. If the ratio of k_x to k_p is sufficiently small so that the locally reacting impedance is the same as the exact line impedance, it can be said that the locally reacting impedance of the plate is valid.

In Figure 3, the relationship between k_x / k_p and the ratio between the two impedances is shown. For $k_x / k_p < 0.5$, the locally reacting impedance is the same as the exact line impedance to within 1 %. Moreover it can also be seen in Figure 4 that k_x / k_p for the structure of Figure 2 has values below 0.3 in the frequency range of interest which is selected as 10 Hz to 1000 Hz. Therefore, the plate can be considered as locally reacting and the general dispersion relation equation (2.18) can be solved by using equation (2.27) for the locally reacting impedance of the plate. This assumption is valid for both the infinite plate and a finite plate considered later.

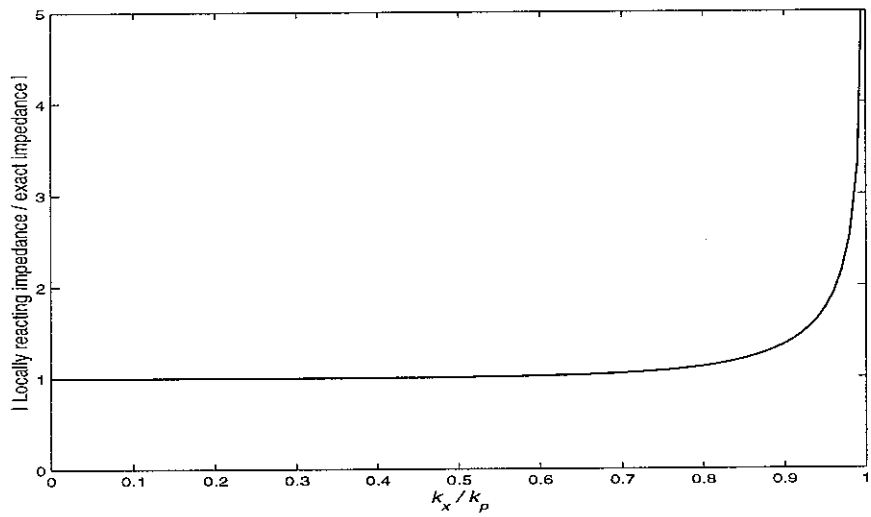

Figure 3. Ratio of the locally reacting impedance to the exact line impedance of the semi-infinite plate.

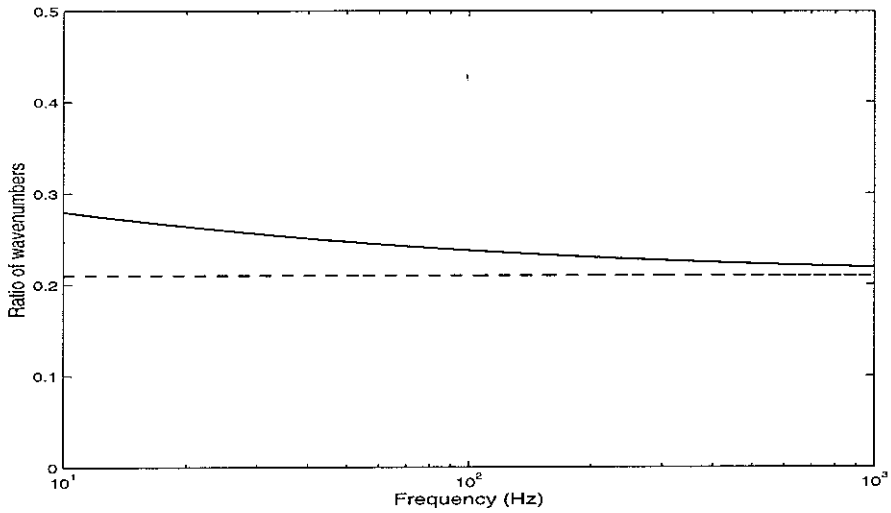

Figure 4. Ratio of wavenumbers. ——: k_x/k_p, — —: k_b/k_p.

Because the wave method is used in the present report, it will be meaningful to understand the characteristics of wavenumbers in the structures. The equations related to the wave method start from basically the free or uncoupled wavenumber of a beam or plate. The coupled beam wavenumber k_x of the built-up structure consisting of a semi-infinite beam and a semi-infinite plate is compared to a semi-infinite beam free wavenumber and a semi-infinite plate free wavenumber in Figure 5.

All of the wavenumbers increase with increasing frequency approximately in proportion to $\omega^{1/2}$ which shows that they are dispersive systems. Because the bending stiffness of the beam is larger than that of the plate, the wavenumber of the plate is greater than that of beam. The ratio of k_b to k_p is also shown in Figure 4 and is constant at 0.209 because both of them are proportional to the square root of the circular frequency. In detail, the coupled wavenumber k_x is a little higher than k_b. The reason can be seen from the dispersion equation (2.18) which includes the impedance term of the plate. The mass of the plate increases k_x, but the influence is reduced at high frequency because the equivalent mass is $m_p''/2k_p$, see equation (2.27). Because of this, as shown in Figure 4, the ratio of k_x to k_p does not have a constant value.

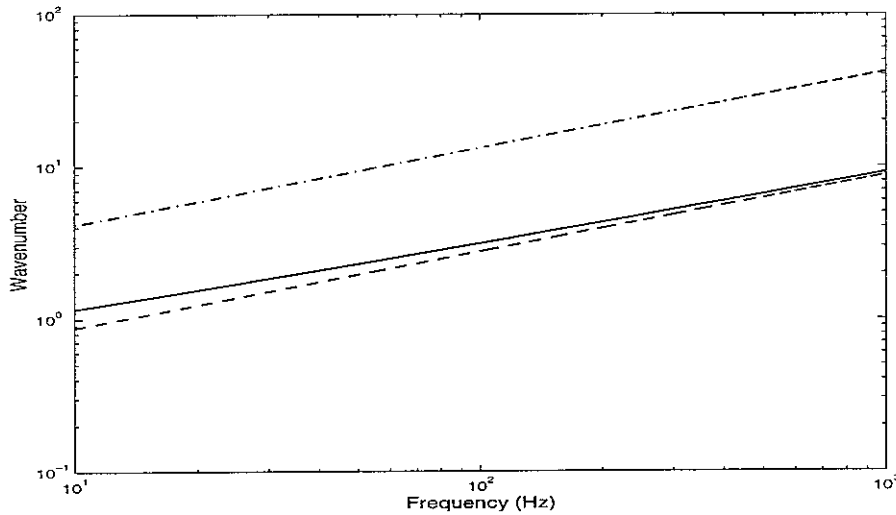

Figure 5. Comparison of the propagating wavenumbers. ———: k_x in the coupled beam as in Figure 2, — —: k_b in an uncoupled semi-infinite beam, — · —: k_p in the plate. k_x is calculated on the basis of the locally reacting plate.

In Figure 6, the ratio of the imaginary part to the real part of the wavenumber k_x is shown. The imaginary part of the wavenumber is related to the damping of the structure. As mentioned in section 2.1, the 'damping' part of the plate impedance makes the coupled wavenumber k_x a complex number. Physically this means that the plate appears to add damping to the spine beam although it does so by energy radiation into the plate (the system is assumed undamped). Figure 6 shows how the damping changes with frequency. An equivalent loss factor η can be derived from equation (2.29) and the ratio shown in Figure 6. It appears to fall with frequency. This tendency was already known by Heckl [13].

$$\frac{\eta}{4} = -\frac{\mathrm{Im}(k_x)}{\mathrm{Re}(k_x)} \tag{2.29}$$

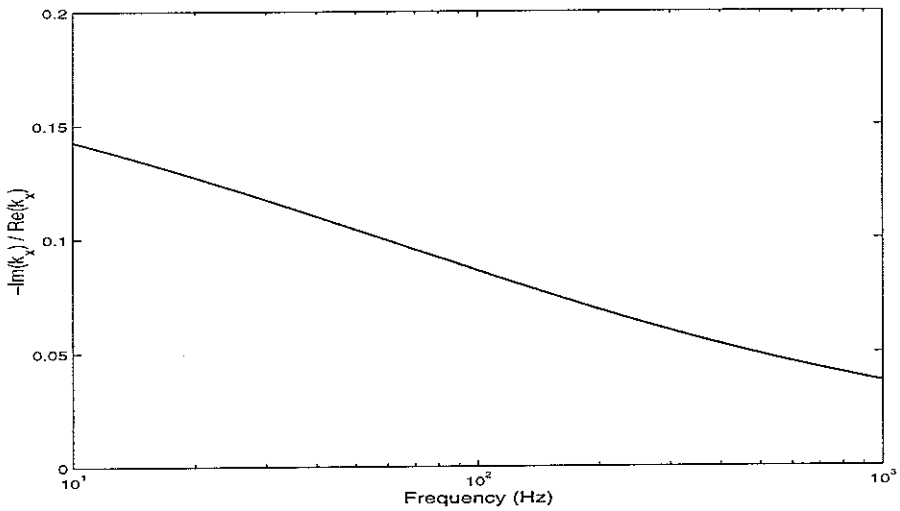

Figure 6. Ratio of the imaginary part to the real part of the wavenumber k_x. k_x is calculated on the basis of the locally reacting plate.

In Figure 7, the locally reacting impedance calculated from equation (2.27) is shown. Because a locally reacting plate has a beam-like nature, the line impedance is similar to that of an infinite beam. The impedance increases with frequency and obviously there are no resonances or anti-resonances due to its infinite extent.

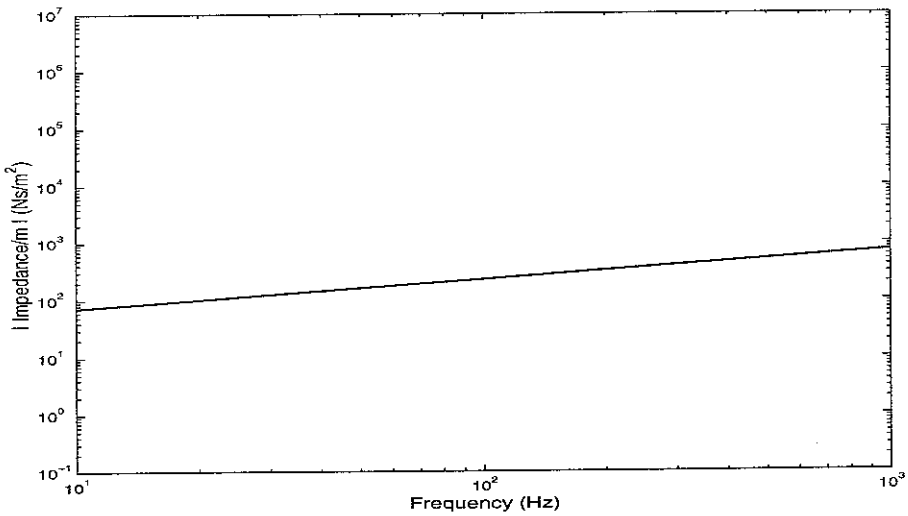

Figure 7. Locally reacting impedance of the semi-infinite plate per unit length of the beam.

In addition to the damping effect of the plate, it would be interesting to see how the dynamic characteristics are changed when damping is introduced to the beam. The beam is given a loss factor 0.05 (see Table 1). In Figure 8, the imaginary part of the wavenumber k_x is shown from which the damping can be inferred. Although the difference is small, it can be seen that the damping is increased.

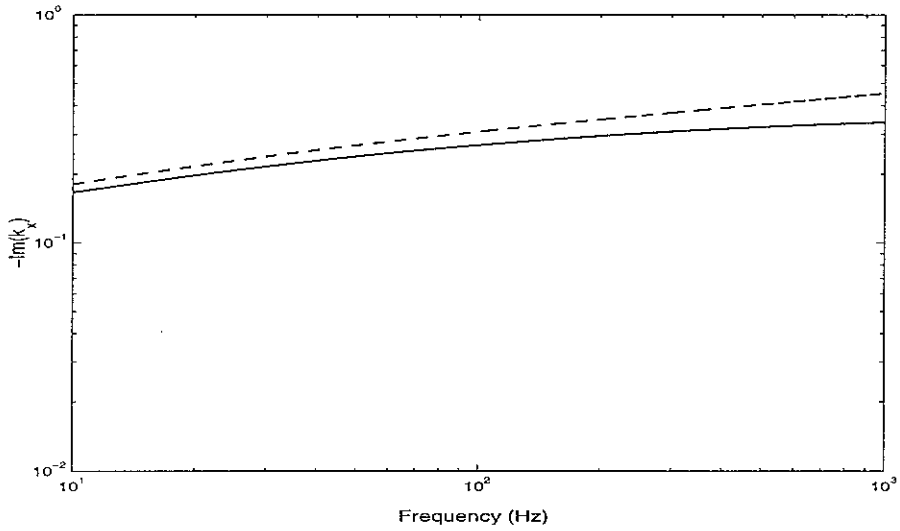

Figure 8. Comparison of the imaginary part of the wavenumber k_x. ——: undamped beam, — —: damped beam.

If damping is included in the beam, the level of the point mobility will be reduced slightly, but as shown in Figure 9, the difference between the solid line and the dashed line (lower two lines) in the mobility graph is not distinguishable. In the phase graph, it can be seen that the dashed line in the upper two lines shows a delayed phase which indicates that the beam includes damping. The point mobility of the structure consisting of the damped semi-infinite beam and the semi-infinite plate is used as a characteristic mobility later in the present report for comparison with the results of different finite structures. Figure 9 also shows the mobility and its phase of an uncoupled semi-infinite beam. Concerning the damping, the tendency is similar to the coupled

beam. Comparing the mobilities between the built-up structure and the uncoupled beam, the built-up structure has a lower level than the uncoupled beam because it is influenced by the mass of the plate. Both fall with increasing frequency which shows a partial mass-like characteristic. The phase of the built-up structure has an increasing delay with frequency because of the damping-like term of the plate while the uncoupled beam has a constant phase of $-\pi/4$.

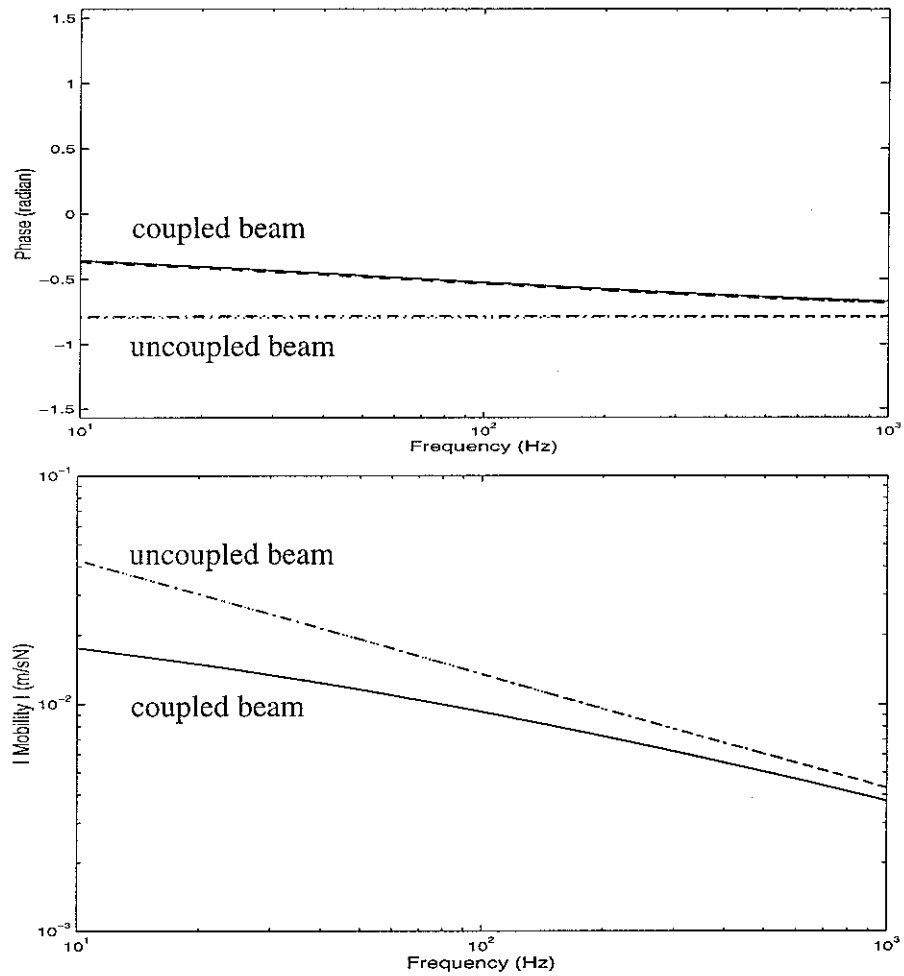

Figure 9. Comparison of the phase and the point mobility. ———: semi-infinite beam and semi-infinite plate as in Figure 2 (undamped beam), — —: semi-infinite beam and semi-infinite plate as in Figure 2 (damped beam), —·—: uncoupled semi-infinite beam (undamped beam), ------: uncoupled semi-infinite beam (damped beam).

3. Infinite beam coupled to finite width plate

3.1 General boundary

This section considers the case shown in Figure 10 in which a plate of finite width is coupled to the beam and the effect of the boundary condition along the opposite edge parallel to the beam is considered in general terms.

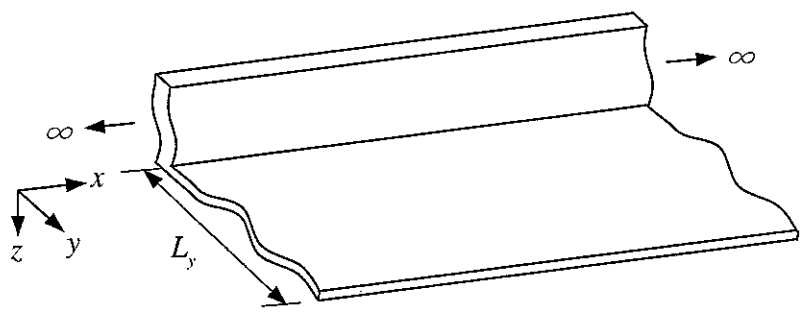

Figure 10. A built-up structure consisting of an infinite beam attached to a finite plate.

If it is assumed that there is no damping in the plate, the response in the infinitely long plate of width L_y joined to an infinitely long beam can be written as

$$\tilde{w}_p = (\tilde{B}e^{-ik_y y} + \tilde{C}e^{-k_e y} + \beta_y \tilde{r}\tilde{B}e^{ik_y y} + \tilde{D}e^{k_e(y-L_y)})e^{-ik_x x} \qquad (3.1)$$

where $\beta_y = e^{-ik_y 2L_y}$ represents a phase shift over length $2L_y$, $\tilde{r}$ is the complex reflection coefficient at the edge of the plate $y = L_y$ and $\tilde{D}$ is the amplitude of the near field wave which is generated at the opposite edge of the plate.

The equation of the motion of the plate is the same as for the semi-infinite plate. At $y = 0$, the boundary conditions in terms of the displacement and force for the finite plate are the same as the semi-infinite plate structure.

From boundary condition ①,

$$\tilde{A} = \tilde{B} + \tilde{C} + \beta_y \tilde{r}\tilde{B} + \tilde{D}e^{-k_e L_y}. \tag{3.2}$$

From boundary condition ②,

$$D_p e^{-ik_x x}\Big[-k_y^2 \tilde{B}e^{-ik_y y} + k_e^2 \tilde{C}e^{-k_e y} - k_y^2 \beta_y \tilde{r}\tilde{B}e^{ik_y y} + k_e^2 \tilde{D}e^{k_e(y-L_y)} - k_x^2 \nu\left(\tilde{B}e^{-ik_y y} + \tilde{C}e^{-k_e y} + \beta_y \tilde{r}\tilde{B}e^{ik_y y} + \tilde{D}e^{k_e(y-L_y)}\right)\Big]_{y=0} = 0.$$

$$-k_y^2 \tilde{B} + k_e^2 \tilde{C} - k_y^2 \beta_y \tilde{r}\tilde{B} + k_e^2 \tilde{D}e^{-k_e L_y} - k_x^2 \nu(\tilde{B} + \tilde{C} + \beta_y \tilde{r}\tilde{B} + \tilde{D}e^{-k_e L_y}) = 0.$$

$$-\left\{k_y^2 + \nu k_x^2\right\}\left(1 + \beta_y \tilde{r}\right)\tilde{B} + \left\{k_e^2 - \nu k_x^2\right\}\tilde{C} + \left\{k_e^2 - \nu k_x^2\right\}\tilde{D}e^{-k_e L_y} = 0. \tag{3.3}$$

Because the beam is attached to the edge $y = 0$ of the plate, at sufficiently high frequency it can be assumed that the influence of the near field at the opposite edge will be negligible, which means $\tilde{D}e^{-k_e L_y} \approx 0$.

Therefore, equations (3.2) and (3.3) become

$$\tilde{A} = (1 + \beta_y \tilde{r})\tilde{B} + \tilde{C} \tag{3.4}$$

and

$$-\left\{k_y^2 + \nu k_x^2\right\}\left(1 + \beta_y \tilde{r}\right)\tilde{B} + \left\{k_e^2 - \nu k_x^2\right\}\tilde{C} = 0. \tag{3.5}$$

Equations (3.4) and (3.5) yield

$$\tilde{C} = \frac{k_y^2 + \nu k_x^2}{k_y^2 + k_e^2} \tilde{A}, \tag{3.6a}$$

$$\tilde{B} = \frac{k_e^2 - \nu k_x^2}{(k_y^2 + k_e^2)(1 + \beta_y \tilde{r})} \tilde{A}. \tag{3.6b}$$

Boundary condition ③ can be rewritten as follows.

$$D_p \frac{\partial}{\partial y}\left(\frac{\partial^2 \tilde{w}_p}{\partial y^2} + (2-\nu)\frac{\partial^2 \tilde{w}_p}{\partial x^2} \right)\Bigg|_{y=0}$$
$$= D_p e^{-ik_x x}\left[ik_y^3 \tilde{B} - k_e^3 \tilde{C} - ik_y^3 \beta_y \tilde{r}\tilde{B} - (2-\nu)k_x^2(-ik_y \tilde{B} - k_e \tilde{C} + ik_y \beta_y \tilde{r}\tilde{B}) \right]$$
$$= D_p e^{-ik_x x}\left[ik_y \left\{ k_y^2 + (2-\nu)k_x^2 \right\}(1 - \beta_y \tilde{r})\tilde{B} - k_e \left\{ k_e^2 - (2-\nu)k_x^2 \right\} \tilde{C} \right] = \tilde{F}(x).$$

Substituting for $\tilde{B}$ and $\tilde{C}$,

$$D_p \tilde{A} e^{-ik_x x}\left[ik_y \frac{\left\{ k_y^2 + (2-\nu)k_x^2 \right\}\left(k_e^2 - \nu k_x^2 \right)(1 - \beta_y \tilde{r})}{(k_y^2 + k_e^2)(1 + \beta_y \tilde{r})} - k_e \frac{\left\{ k_e^2 - (2-\nu)k_x^2 \right\}\left(k_y^2 + \nu k_x^2 \right)}{(k_y^2 + k_e^2)} \right] = \tilde{F}(x). \tag{3.7}$$

Therefore, the line impedance is given by

$$\tilde{Z}_p' = \frac{D_p}{\omega}\left[\frac{k_y \left\{ k_y^2 + (2-\nu)k_x^2 \right\}\left(k_e^2 - \nu k_x^2 \right)(1 - \beta_y \tilde{r}) + ik_e \left\{ k_e^2 - (2-\nu)k_x^2 \right\}\left(k_y^2 + \nu k_x^2 \right)(1 + \beta_y \tilde{r})}{(k_y^2 + k_e^2)(1 + \beta_y \tilde{r})} \right] \tag{3.8}$$

3.2 Simply supported boundary

For a simply supported condition as shown in Figure 11, the reflection coefficient $\tilde{r}$ becomes –1, which means that propagating waves undergo a phase shift of π.

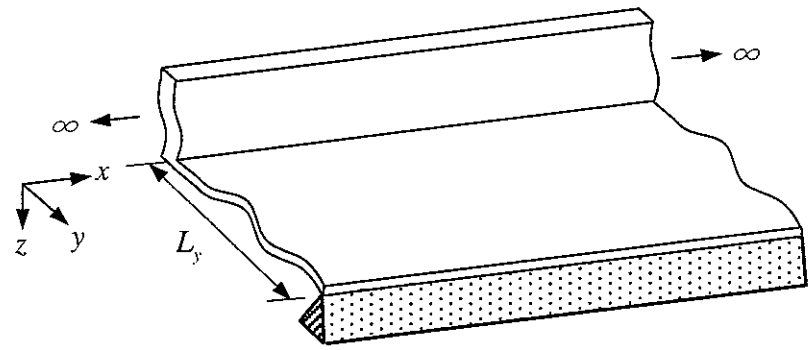

Figure 11. A built-up structure consisting of an infinite beam attached to a finite plate with simply supported edge.

Therefore, equation (3.8) becomes

$$\tilde{Z}'_p = \frac{D_p}{\omega}\left[\frac{k_y\left\{k_y^2+(2-\nu)k_x^2\right\}\left(k_e^2-\nu k_x^2\right)\left(1+\beta_y\right)+ik_e\left\{k_e^2-(2-\nu)k_x^2\right\}\left(k_y^2+\nu k_x^2\right)(1-\beta_y)}{(k_y^2+k_e^2)(1-\beta_y)}\right]. \tag{3.9}$$

3.3 Approximation by locally reacting impedance

Because the relationship between the wavenumbers k_p, k_x, k_y and k_e is the same as for the semi-infinite plate structure, the impedance can be written as follows.

$$\tilde{Z}'_p = \frac{D_p}{\omega}\left[\frac{k_y\left\{k_p^2+(1-\nu)k_x^2\right\}^2\left(1+\beta_y\right)+ik_e\left\{k_p^2-(1-\nu)k_x^2\right\}^2(1-\beta_y)}{2k_p^2(1-\beta_y)}\right]. \tag{3.10}$$

If $k_p >> k_x$, then $k_e \approx k_p$, $k_y \approx k_p$, and

$$\begin{aligned}\tilde{Z}'_p\big|_{k_p>>k_x} &= \frac{D_p}{\omega}\left[\frac{k_p^5\left\{1+(1-\nu)k_x^2/k_p^2\right\}^2\left(1+\beta_y\right)+ik_p^5\left\{1-(1-\nu)k_x^2/k_p^2\right\}^2(1-\beta_y)}{2k_p^2(1-\beta_y)}\right] \\ &\approx \frac{D_p k_p^3(1+\beta_y+i-i\beta_y)}{2\omega(1-\beta_y)}.\end{aligned} \tag{3.11}$$

Therefore, the line impedance of the plate can be expressed in the simple form of

$$\tilde{Z}'_p\Big|_{k_p>>k_x} \approx \frac{D_p k_p^3}{2\omega}\left(\frac{1+\beta_y}{1-\beta_y}+i\right) \tag{3.12}$$

where β_y depends on k_y. The wavenumber relationship between the real values k_y, k_p, and k_x are still satisfied which is

$$k_y = \sqrt{k_p^2 - k_x^2}\,. \tag{3.13}$$

where k_y could be found iteratively from equation (3.12) and the dispersion relation.

3.4 Effect of damping

If damping is introduced into the plate, the plate stiffness is described as $\tilde{D}_p = D_p(1+i\eta_p)$ and the wavenumber of the plate becomes $\tilde{k}_p \approx k_p(1-i\eta_p/4)$.

Now, equation (3.12) which represents the locally reacting impedance of the plate, can be given as follows including damping terms.

$$\tilde{Z}'_p\Big|_{k_p>>k_x} \approx \frac{\tilde{D}_p \tilde{k}_p^3}{2\omega}\left(\frac{1+\tilde{\beta}_y}{1-\tilde{\beta}_y}+i\right)\,. \tag{3.14}$$

where $\tilde{\beta}_y = e^{-i\tilde{k}_y 2L_y}$ is the propagating wave attenuation coefficient of the plate, which represents attenuation as well as phase shift over the length $2L_y$.

Once the damping is introduced to the beam and the plate, strictly their wavenumber matching cannot be satisfied because each wavenumber includes a damping term. Nevertheless, if the loss factor of the spine can be assumed to be very small, then because the spine wavenumber k_x is

smaller than k_p, the receiver wavenumber $\tilde{k}_y$ can be calculated in terms of the loss factor of the plate as follows.

$$\tilde{k}_y \approx k_y\left(1-i\frac{\eta_p}{4}\right) \tag{3.15}$$

3.5 Numerical analysis

Computer simulations were carried out for a semi-infinite beam as in section 2.5. Figure 12 shows the built-up structure consisting of the semi-infinite beam and the plate which has finite width L_y. For the plate both damped and undamped cases are considered but the beam has damping for both cases.

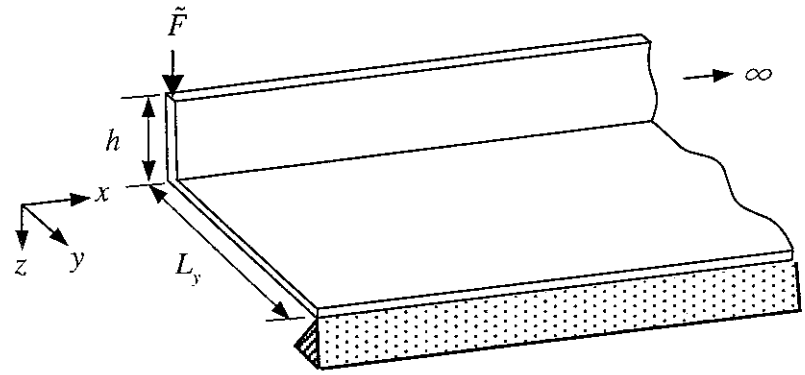

Figure 12. A built-up structure consisting of a semi-infinite beam attached to a finite plate with a simply supported edge.

The configuration considered for the built-up structure shown in Figure 12 is presented in Table 2. The material properties are the same as those presented in Table 1 as are the thicknesses. A point force was applied at the same location $x = 0$.

Table 2. Dimensions of the built-up structure shown in Figure 12.

Plate width, L_y (m)	0.45
Thickness, t (mm)	5.9
Height of the beam, h (mm)	68.0
Loss factor of the beam, η_b	0.05
Loss factor of the plate (if used), η_p	0.05

Firstly, the impedance of the undamped plate calculated from equation (3.12) is shown in Figure 13. The resonances (dips) and anti-resonances (peaks) actually tend to $\pm\infty$ but this is truncated by the frequency resolution used which is 0.1 Hz. It can be seen that there are erratic fluctuations near the anti-resonances. This is due to β_y including the propagating wavenumber k_y, which is also related to the coupled wavenumber k_x (see equation (3.13)). Note that for an undamped plate, β_y does not include an attenuation term.

Figure 14 shows the point mobility of the built-up structure shown in Figure 12. It was calculated using the impedance shown in Figure 13 and the general dispersion equation, when the semi-infinite beam of the structure has damping loss factor 0.05. The point mobility is shown along with the characteristic mobility of Figure 9. It can be seen that the point mobility follows the characteristic mobility well.

Because a semi-infinite beam has no resonances or anti-resonances, the dynamic characteristics of the built-up structure will be determined by the characteristics of the plate. It seems to be important to notice that the peaks in Figure 13 and the dips in Figure 14 occur at the same frequencies. The peaks in the impedance correspond to the anti-resonances, and at these

anti-resonance frequencies of the plate the point mobility level of the built-up structure is minimized. This phenomenon will be explained later.

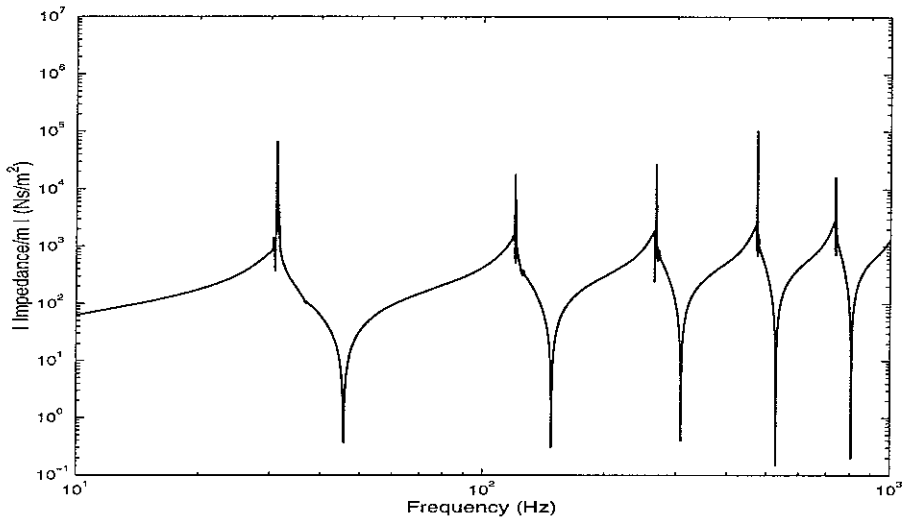

Figure 13. Locally reacting impedance of the finite plate (undamped plate).

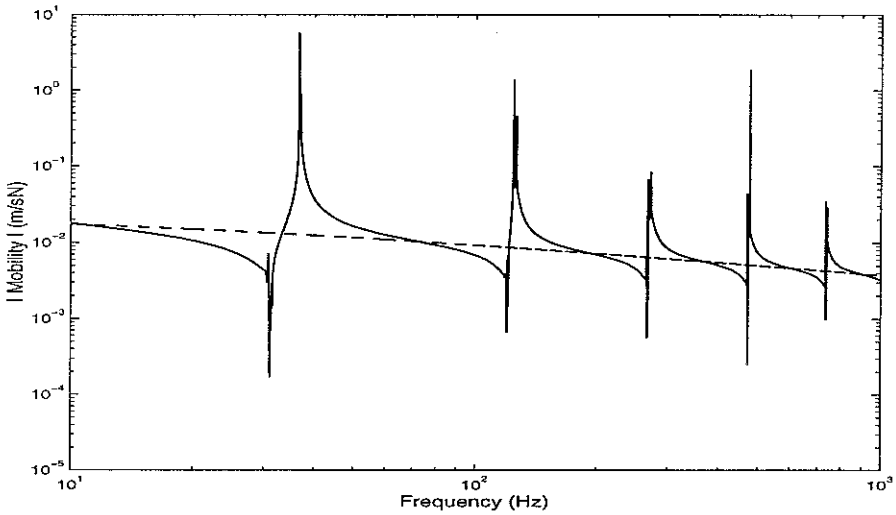

Figure 14. Point mobility of the built-up structure. ——: finite width plate as in Figure 12 (undamped plate, $\eta_b = 0.05$ in the beam, point force applied at $x = 0$), — —: infinite plate as in Figure 2 (undamped plate, $\eta_b = 0.05$ in the beam, point force applied at $x = 0$).

For the case where damping is added to the plate, the various wavenumbers are compared in Figure 15. This shows the propagating wavenumber k_y, the near field wavenumber k_e and the free wavenumber k_p along with k_x. As k_p is larger than k_x, the difference between k_p, k_y, and k_e is small. This means that k_p can be used in the calculation of the plate impedance instead of k_y and k_e (see equations (3.12) and (3.10)).

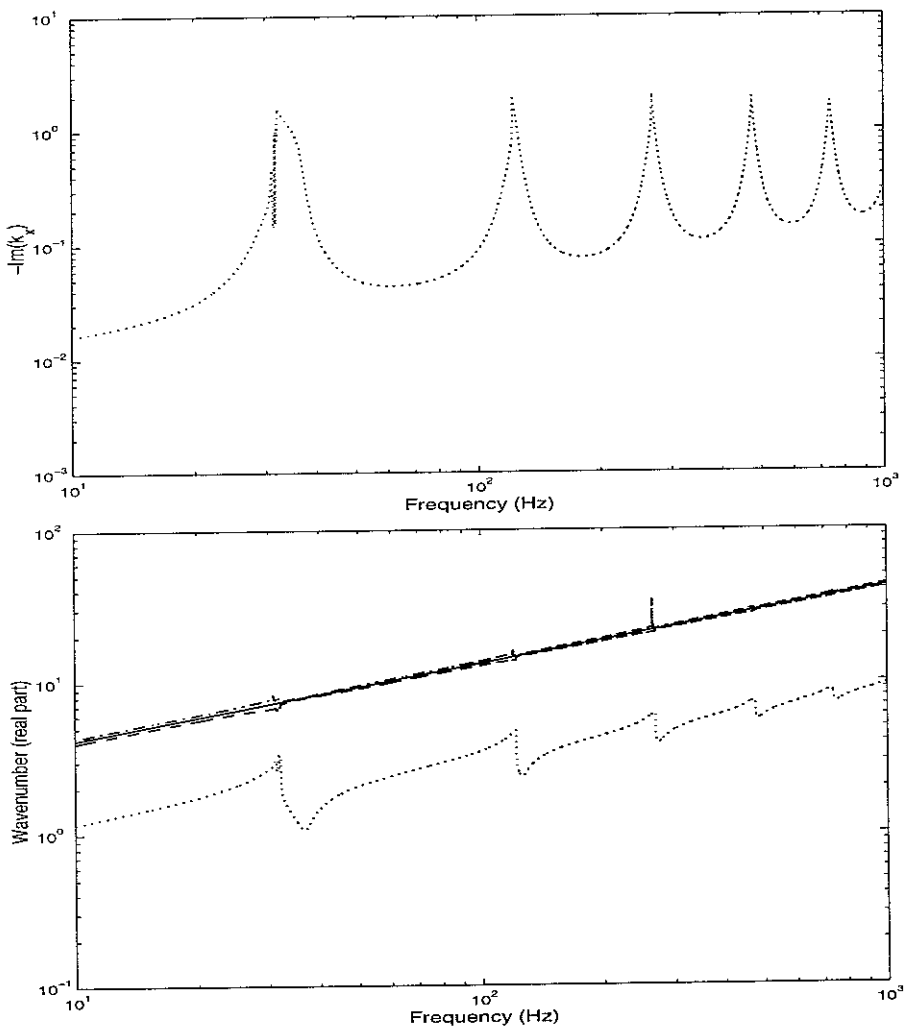

Figure 15. Comparison of the wavenumber of the built-up structure consisting of the semi-infinite beam and the finite plate as in Figure 12. ——: k_p, — —: k_y, —·—: k_e, -------: k_x.

Also, the imaginary part of the coupled wavenumber k_x is shown in Figure 15. As mentioned in section 2.5, the imaginary part is related to the damping of the structure. When the imaginary part of the coupled wavenumber is divided by the real part, it is possible to infer an equivalent loss factor. This ratio is shown in Figure 16, which according to equation (2.29) indicates beam loss factors greater than 1 at the first few peaks.

For the comparison, the impedance of the damped plate is shown in Figure 17, calculated using equation (3.14). From comparing Figure 16 and 17, it is clear that the equivalent loss factor is maximum at anti-resonance frequencies of the plate.

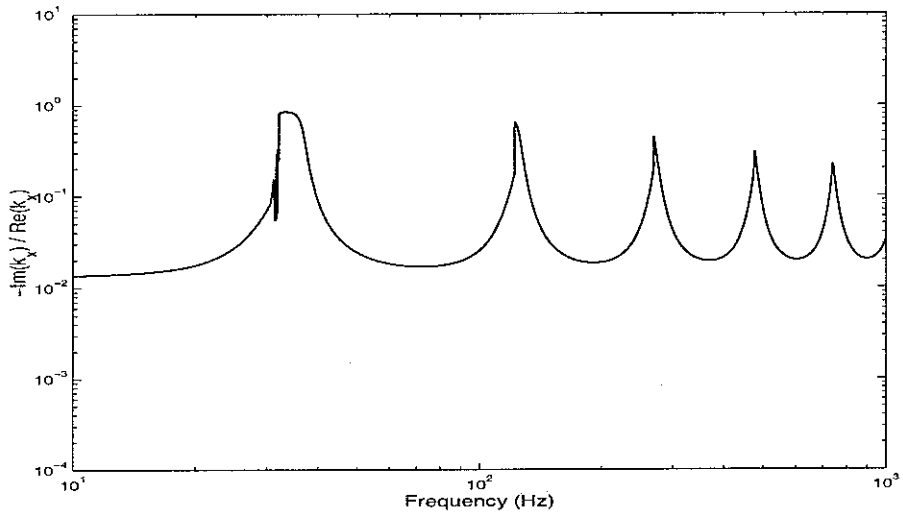

Figure 16. Ratio of the imaginary part to the real part of the wavenumber $\tilde{k}_x$.

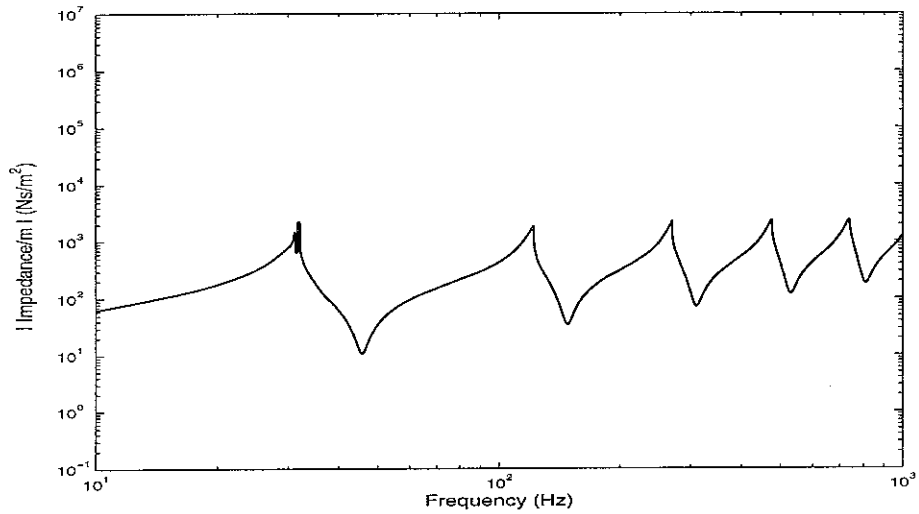

Figure 17. Locally reacting impedance of the finite plate ($\eta_p = 0.05$ in the plate).

It can be seen that there are erratic fluctuations in both figures near the first anti-resonance. This is again becuase of the influence of $\tilde{\beta}_y$. At high frequencies the fluctuations seen earlier disappear due to the attenuation of the propagating wave in the plate which increases at higher frequency.

In addition to the impedance of the damped plate, the corresponding point mobility of the built-up structure is shown in Figure 18. Similar to the undamped plate in Figure 14, the anti-resonance frequencies of the plate, such as 31.9, 122.0, 269.8, 474.9, and 736.7 Hz coincide with the dips of the point mobility of the coupled structure. This can be explained by the equivalent loss factor mentioned above. Therefore, the motion of the coupled beam is reduced at anti-resonances of the plate.

Comparing Figures 14 and 18, it can be seen that the damping of the plate has an obvious influence on the drive point mobility of the beam, reducing both peaks and troughs.

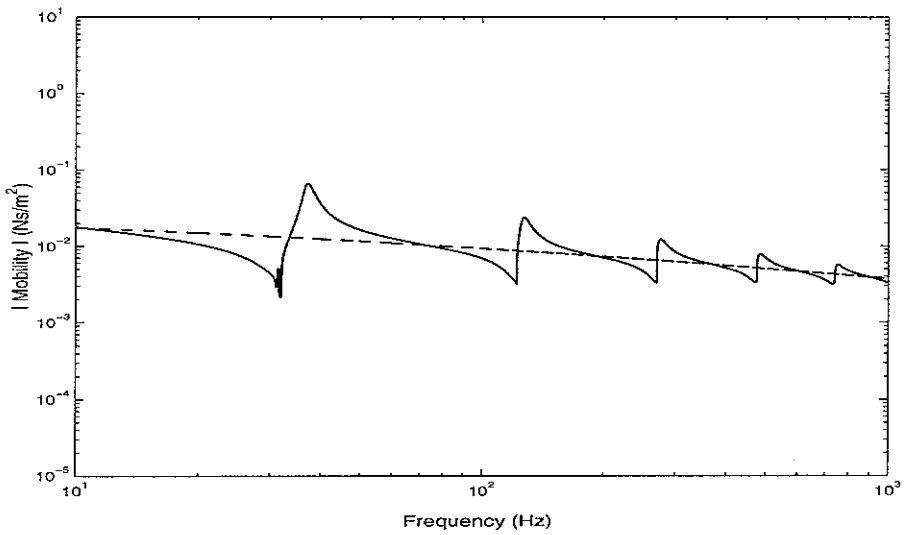

Figure 18. Point mobility of the built-up structure. ——: finite width plate as in Figure 12 ($\eta_p = 0.05$ in the plate, $\eta_b = 0.05$ in the beam, point force applied at x = 0), — —: infinite plate as in Figure 2 (undamped plate, $\eta_b = 0.05$ in the beam, point force applied at $x = 0$).

4. Finite beam coupled to finite plate

4.1 Response of coupled system

To define the dispersion relationships of a coupled beam and plate, an infinite beam and a plate of either infinite or finite width were used in the previous sections. This general relationship can be extended to the structure which is finite in length as shown in Figure 19. In addition, based on equations for the transfer mobility and the point mobility of the finite beam, the point mobility as well as the transfer mobility of the built-up structure can be calculated using the corresponding propagation and near field wavenumber of the built-up structure.

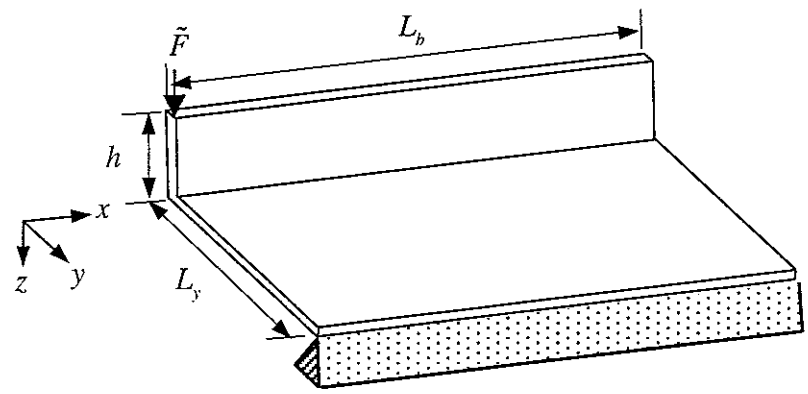

Figure 19. A built-up structure consisting of a finite beam attached to a finite plate with a simply supported edge.

The general solution for the motion of the finite beam of the built-up structure at frequency ω is

$$\tilde{w} = \tilde{A}_1 e^{-i\tilde{k}_x x} + \tilde{A}_2 e^{-\tilde{k}_{nf} x} + \tilde{A}_3 e^{i\tilde{k}_x x} + \tilde{A}_4 e^{\tilde{k}_{nf} x} \tag{4.1}$$

where $\tilde{A}_1$ and $\tilde{A}_3$ are the amplitudes of propagating waves, $\tilde{A}_2$ and $\tilde{A}_4$ are the amplitudes of the near field waves, $\tilde{k}_x$ is the propagating wavenumber and $\tilde{k}_{nf}$ is the near field wavenumber of the coupled beam in a complex number (allowing for damping).

If the beam has length l with a force $\tilde{F}$ applied at one end $x = 0$, and is free at both ends, the boundary conditions are then given by

$$\tilde{D}_b \left. \frac{\partial^2 \tilde{w}}{\partial x^2} \right|_{x=0} = 0, \tag{4.2a}$$

$$-\tilde{D}_b \left. \frac{\partial^3 \tilde{w}}{\partial x^3} \right|_{x=0} = \tilde{F}, \tag{4.2b}$$

$$\tilde{D}_b \left. \frac{\partial^2 \tilde{w}}{\partial x^2} \right|_{x=l} = 0, \tag{4.2c}$$

$$\tilde{D}_b \left. \frac{\partial^3 \tilde{w}}{\partial x^3} \right|_{x=l} = 0. \tag{4.2d}$$

Equations (4.2) also can be written in terms of the wave amplitudes:

$$-k_x^2 \tilde{A}_1 + k_{nf}^2 \tilde{A}_2 - k_x^2 \tilde{A}_3 + k_{nf}^2 \tilde{A}_4 = 0, \tag{4.3}$$

$$-\tilde{D}_b (ik_x^3 \tilde{A}_1 - k_{nf}^3 \tilde{A}_2 - ik_x^3 \tilde{A}_3 + k_{nf}^3 \tilde{A}_4) = \tilde{F}, \tag{4.4}$$

$$-k_x^2 e^{-i\tilde{k}_x l} \tilde{A}_1 + k_{nf}^2 e^{-\tilde{k}_{nf} l} \tilde{A}_2 - k_x^2 e^{i\tilde{k}_x l} \tilde{A}_3 + k_{nf}^2 e^{\tilde{k}_{nf} l} \tilde{A}_4 = 0, \tag{4.5}$$

$$ik_x^3 e^{-i\tilde{k}_x l} \tilde{A}_1 - k_{nf}^3 e^{-\tilde{k}_{nf} l} \tilde{A}_2 - ik_x^3 e^{i\tilde{k}_x l} \tilde{A}_3 + k_{nf}^3 e^{\tilde{k}_{nf} l} \tilde{A}_4 = 0. \tag{4.6}$$

These can be written in a matrix form,

$$\begin{bmatrix} -k_x^2 & k_{nf}^2 & -k_x^2 & k_{nf}^2 \\ -ik_x^3 & k_{nf}^3 & ik_x^3 & -k_{nf}^3 \\ -k_x^2 e^{-i\tilde{k}_x l}{}_1 & k_{nf}^2 e^{-\tilde{k}_{nf} l} & -k_x^2 e^{i\tilde{k}_x l} & k_{nf}^2 e^{\tilde{k}_{nf} l} \\ ik_x^3 e^{-i\tilde{k}_x l} & -k_{nf}^3 e^{-\tilde{k}_{nf} l} & -ik_x^3 e^{i\tilde{k}_x l} & k_{nf}^3 e^{\tilde{k}_{nf} l} \end{bmatrix} \begin{Bmatrix} \tilde{A}_1 \\ \tilde{A}_2 \\ \tilde{A}_3 \\ \tilde{A}_4 \end{Bmatrix} = \begin{Bmatrix} 0 \\ \tilde{F}/\tilde{D}_b \\ 0 \\ 0 \end{Bmatrix}. \tag{4.7}$$

Therefore, when the propagating wavenumber and the near field wavenumber are known, the amplitudes of the waves can be found by inverting the matrix. Strictly, the propagating wave and the near field wave should be calculated separately, but as mentioned in section 2.4, the theoretical development in the present report is based on the propagating wave in a coupled beam. Therefore, the near field wavenumber is assumed to have the same value as the propagating wavenumber based on the locally reacting plate impedance and the general dispersion relation.

Now equations (4.3) ~ (4.6) can be simplified using $\tilde{k}_x$ instead of $\tilde{k}_{nf}$ and the amplitudes $\tilde{A}_2$, $\tilde{A}_3$, and $\tilde{A}_4$ can be derived in terms of $\tilde{A}_1$.

$$\tilde{A}_3 = \left(\frac{-(1+i) + ie^{-i\tilde{k}_x l} e^{\tilde{k}_x l} + e^{-i\tilde{k}_x l} e^{-\tilde{k}_x l}}{(1+i) - ie^{i\tilde{k}_x l} e^{-\tilde{k}_x l} - e^{i\tilde{k}_x l} e^{\tilde{k}_x l}} \right) \tilde{A}_1 . \tag{4.8}$$

$$\tilde{A}_2 = \left(\frac{1+i}{2} e^{-ik_x l} \tilde{A}_1 + \frac{1-i}{2} e^{ik_x l} \tilde{A}_3 \right) e^{k_x l} . \tag{4.9}$$

$$\tilde{A}_4 = \left(\frac{1-i}{2} e^{-ik_x l} \tilde{A}_1 + \frac{1+i}{2} e^{ik_x l} \tilde{A}_3 \right) e^{-k_x l} . \tag{4.10}$$

Therefore, the transfer mobility from the excitation point $x = 0$ to the response at the arbitrary position x can be calculated from the relationship between equations (4.1) and (4.4), i.e. the relationship between the force and velocity,

$$\tilde{Y}(x) = \frac{i\omega\tilde{w}}{\tilde{F}} = \frac{\omega}{-\tilde{D}_b \tilde{k}_x^{\,3}} \frac{\tilde{A}_1 e^{-i\tilde{k}_x x} + \tilde{A}_2 e^{-\tilde{k}_x x} + \tilde{A}_3 e^{i\tilde{k}_x x} + \tilde{A}_4 e^{\tilde{k}_x x}}{\tilde{A}_1 + i\tilde{A}_2 - \tilde{A}_3 - i\tilde{A}_4} . \tag{4.11}$$

This also gives the point mobility at $x = 0$ as follows.

$$\tilde{Y}_0 = \frac{\omega}{-\tilde{D}_b \tilde{k}_x^{\,3}} \frac{\tilde{A}_1 + \tilde{A}_2 + \tilde{A}_3 + \tilde{A}_4}{\tilde{A}_1 + i\tilde{A}_2 - \tilde{A}_3 - i\tilde{A}_4} . \tag{4.12}$$

4.2 Power input to coupled system

The total power injected into the coupled beam-plate structure by the point force applied at the end is given by

$$P_{total} = \frac{1}{2} \mathrm{Re}\left\{ \tilde{F}_0 \, \tilde{v}_0^* \right\} = \frac{1}{2} \left| \tilde{F}_0 \right|^2 \mathrm{Re}\left\{ \tilde{Y}_0 \right\} \tag{4.13}$$

where $\tilde{Y}_0$ is the input point mobility of the coupled structure driven by the point force, given by equation (4.12).

4.3 Power transmitted to plate

As mentioned in section 2.4, if the plate wavenumber is at least twice the coupled beam wavenumber, the plate can be regarded as locally reacting. With this assumption that the plate can be represented by a locally reacting impedance, the plate behaves like separate strips as shown in Figure 20, because the wave radiated into the plate has a direction almost normal to the axis of the beam.

The power flowing into a structure can be calculated based on its impedance and the velocity at the connection point.

$$P = \frac{1}{2} |\tilde{v}_0|^2 \, \mathrm{Re}\{\tilde{Z}'\} \tag{4.14}$$

In this section the power transmitted to the plate is evaluated and compared to the total power input to the coupled structure by the point force.

The response of the beam to a point force can be written in terms of transfer mobilities for the positions shown in Figure 20. Therefore, the velocity of the plate strips at their attachment points becomes

$$\tilde{v}_0 = \tilde{Y}_{b,0}\tilde{F}_0, \quad \tilde{v}_1 = \tilde{Y}_{b,1}\tilde{F}_0, \quad \tilde{v}_2 = \tilde{Y}_{b,2}\tilde{F}_0, \cdots \tag{4.15}$$

where $\tilde{Y}_{b,x}$ is the transfer mobility $\tilde{Y}_b(x)$ of the coupled beam.

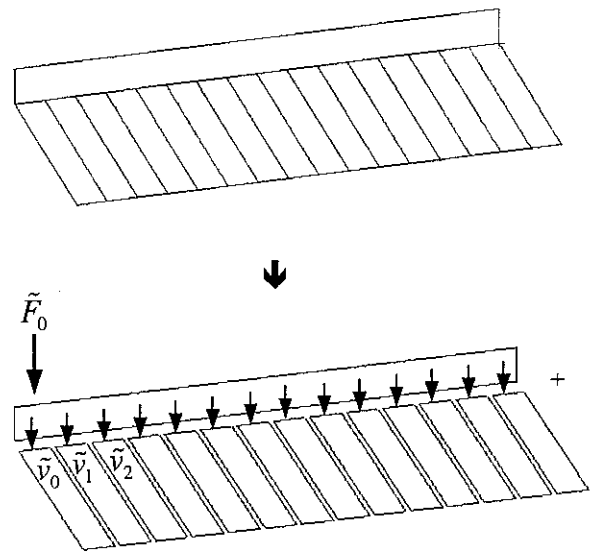

Figure 20. Power flow from a beam to strips of a plate.

The impedance per unit length of a locally reacting finite width plate is defined in section 3.4 and given by

$$\tilde{Z}'_p = \frac{\tilde{D}_p \tilde{k}_p^3}{2\omega}\left(\frac{1+\tilde{\beta}_y}{1-\tilde{\beta}_y}+i\right). \tag{4.16}$$

Now, it is possible to assume that the strip is being driven by a prescribed velocity distribution. Therefore, using equation (4.14), (4.15) and (4.16), the power input into a strip of the plate of width dx can be calculated as follows.

$$P_{strip} = \frac{1}{2}\left|\tilde{v}_x\right|^2 \mathrm{Re}\left\{\tilde{Z}'_p\right\}dx = \frac{1}{2}\left|\tilde{F}_0\right|^2 \left|\tilde{Y}_b(x)\right|^2 \mathrm{Re}\left\{\tilde{Z}'_p\right\}dx. \tag{4.17}$$

Finally, the power input to the plate can be obtained from the integral of equation (4.17) over the length of the beam and is given by

$$P_{plate} = \int_0^l P_{strip}\, dx = \frac{1}{2}\left|F_0\right|^2 \mathrm{Re}\left\{\tilde{Z}'_p\right\} \int_0^l \left|\tilde{Y}_b(x)\right|^2 dx. \tag{4.18}$$

4.4 Numerical analysis

For the built-up structure consisting of a finite beam attached to a finite plate shown in Figure 19, some results from the numerical analysis are shown. Dimensions of the structure are given in Table 3. The results of the analysis are compared to those obtained by a finite element analysis. Figure 21 shows the FE model. Damping is included with FE model by a modal damping ratio which is equivalent to a loss factor as follows.

$$\zeta = \frac{\eta}{2} \tag{4.19}$$

Table 3. Dimensions of the built-up structure shown in Figure 19.

Beam length, L_b (m)	2.0
Plate width, L_y (m)	0.45
Thickness, t (mm)	5.9
Height of the beam, h (mm)	68.0
Loss factor of the beam, η_b	0.05
Loss factor of the plate, η_p	0.05

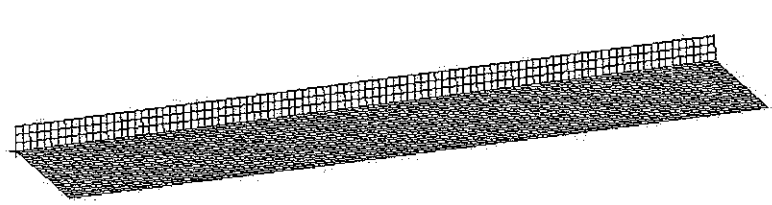

Figure 21. FE model for comparison with numerical analysis.

The point mobility is compared to the characteristic mobility in Figure 22. As in section 3.5, the point mobility follows the characteristic mobility. Some of the peaks correspond to modes of the finite beam, but the second, fifth and eighth peaks, for example, correspond to peaks in the mobility of the infinite beam and finite plate structure in Figure 18. Figure 23 shows the transfer mobility of the built-up structure from $x = 0$ to a response at $x = 2\,\mathrm{m}$, the opposite end of the beam. It can be seen that there are some deep troughs at 31.9, 122.0, 269.8, 474.9, and 736.7 Hz. Comparing Figure 23 with Figure 17, the frequencies of these troughs coincide exactly with the anti-resonances of the finite width plate. This is due to the same reason as explained in section 3.5. That is, the anti-resonance of the plate reduces the vibration along the beam at that frequency. This phenomenon is referred to as a 'blocking effect' in [11].

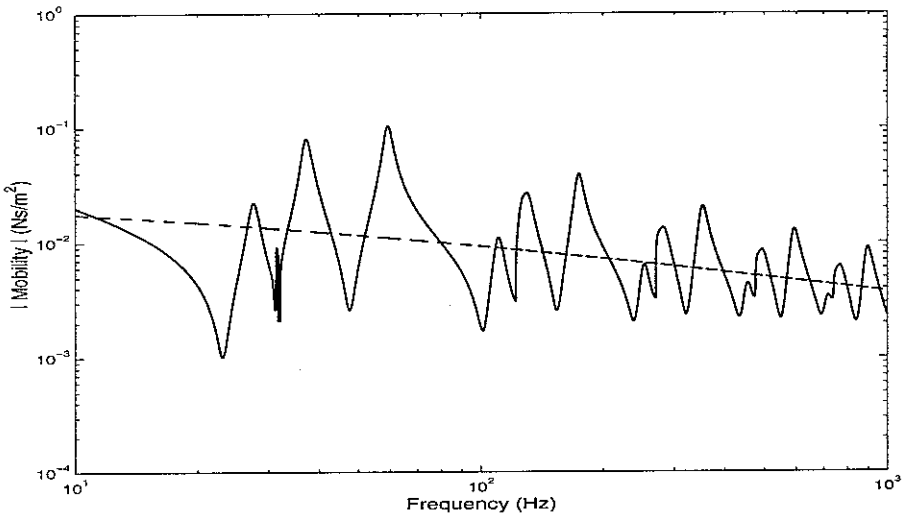

Figure 22. Point mobility of the built-up structure. ———: finite beam and finite plate as in Figure 19 ($\eta_p = 0.05$ in the plate, $\eta_b = 0.05$ in the beam, point force applied at x = 0), — —: infinite beam and infinite plate as in Figure 2 (undamped plate, $\eta_b = 0.05$ in the beam, point force applied at x = 0).

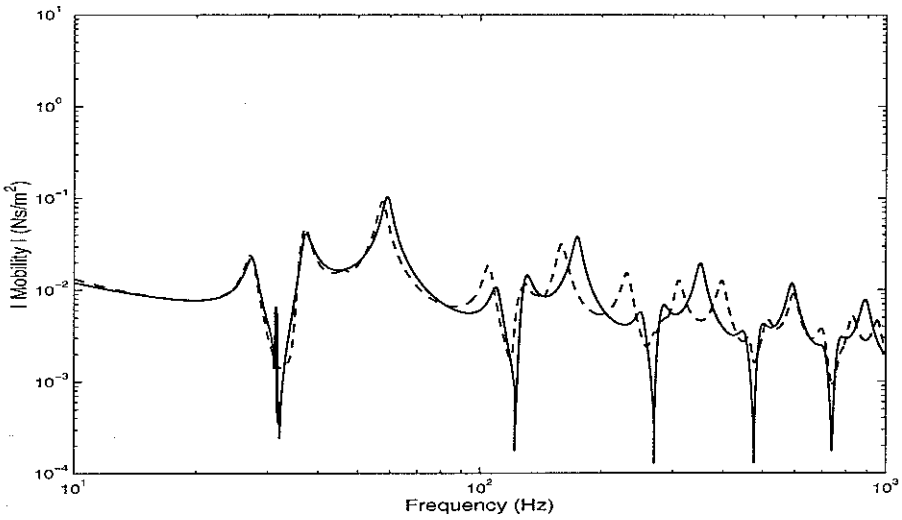

Figure 23. Transfer mobility of the built-up structure consisting of finite beam and finite plate as in Figure 19 ($\eta_p = 0.05$ in the plate, $\eta_b = 0.05$ in the beam, point force applied at x = 0, response at $x = 2.0$). ———: analysis, — —: FEM.

The transfer mobility and the point mobility from the simulations are compared to corresponding results from the finite element analysis in Figures 23 and 24. Below 100 Hz, they agree closely. Above 100 Hz, although the general tendency of the curves coincides well, the resonance frequencies show differences. The main reason for these differences seems to be due to the approximation of the neutral axis of the beam. As mentioned in section 2.5, the bending stiffness of the beam is calculated on the assumption that the neutral axis lies in the mid-plane of the plate. This is basically a good approximation for the fundamental modes of the beam motion, for example, a rigid mode or first bending mode, but for more complicated modes at higher frequencies, it seems that the neutral axis does not lie in the mid-plane of the plate any more because the spine beam is much stiffer than the plate. This can be easily verified from a different finite element model.

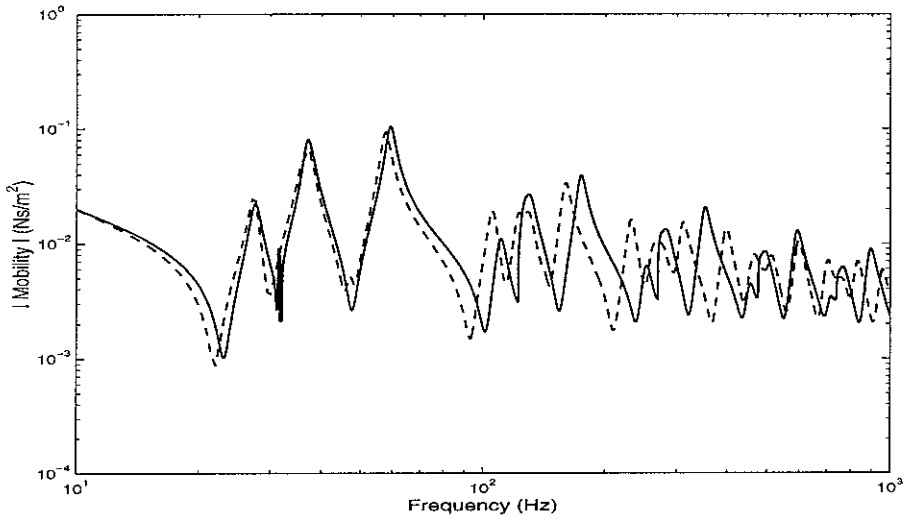

Figure 24. Point mobility of the built-up structure consisting of finite beam and finite plate as in Figure 19 ($\eta_p = 0.05$ in the plate, $\eta_b = 0.05$ in the beam, point force applied at x = 0). ——: analysis, — —: FEM.

Figure 25 shows the modified model in which the plate is attached at the centre of the beam height. In this model, the neutral axis lies at the centre of the beam and will not change for different modes. Figure 26 shows the results of the finite element analysis and the numerical analysis in which the neutral axis also lies at the centre of the beam. The resonance frequencies coincide well. Therefore, if a plate is attached to the bottom of a beam, it is necessary to calculate the neutral axis of the beam using a more accurate method to describe the real dynamic behaviour. This requires further study.

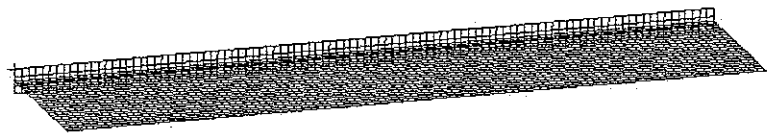

Figure 25. FE model for comparison with numerical analysis (the plate is attached to the centre of the beam height).

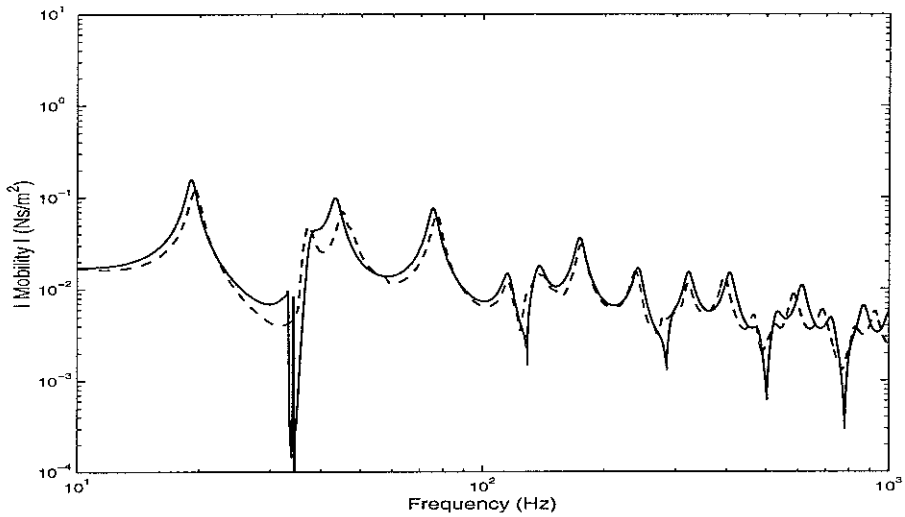

Figure 26. Transfer mobility of the built-up structure consisting of finite beam and finite plate, when the finite plate is attached to the centre of the beam height ($\eta_p = 0.05$ in the plate, $\eta_b = 0.05$ in the beam, point force applied at x = 0, response at x = 2.0). ——: analysis, — —: FEM.

The power distribution for the structure of Figure 19 was calculated using the equations in section 4.3 and 4.4 and is displayed in Figure 27. As expected, the total input power for the structure is greater than the power transferred to the plate. Comparing the point mobility of the

built-up structure, shown in Figure 22 and the power, it is clear that the power is maximum at the resonances of the built-up structure.

While at some peaks such as at 37.1, 128.8, 277.1, 484.1, and 751.5 Hz, the total power and the power transferred to the plate have almost same values, at other peaks such as at 59.0, 174.0, 351.0, 589.7, and 890.1 Hz, the difference between the two powers is large. This could be explained in terms of mode shapes of the beam and the plate. Although the modes of the beam and the plate are coupled, nevertheless, at some natural frequencies the mode of the beam is dominant, at other frequencies the mode of the plate is dominant. Therefore, it can be said that when the difference between the two powers is reduced, the mode of the plate is dominant and the plate receives most energy. In that case, the magnitude of the beam motion is relatively small. Conversely, if the difference is large, the magnitude of the beam motion becomes larger than that of the plate. For example, at 59.0 Hz, the dominant mode of the built-up structure is flexural mode of the beam with two nodes and the 3 noded flexural mode is dominant at 174.0 Hz.

The ratio of the power transferred to the plate, or power dissipated by the plate, to the total input power is shown in Figure 28. When the ratio has the value of 1, all of the total power is transferred to the plate. As seen in the figure, at some specific frequencies such as 31.9, 122.0, 269.8, 474.9, and 736.7 Hz, most of the power is transferred to the plate, and those frequencies coincide with the anti-resonance frequencies of the plate. These frequencies are just below the corresponding resonance of the coupled system that is dominated by plate motion. The total power level is reduced at these plate anti-resonance frequencies as seen in Figure 27. Therefore, when the plate is in anti-resonance, it can be said that most power is transferred to the plate. This is due to the blocking effect mentioned above. Because at those frequencies the plate absorbs the power, it is known that a flexible finite plate can be used as a narrow band vibration damper which absorbs the vibrational energy [11].

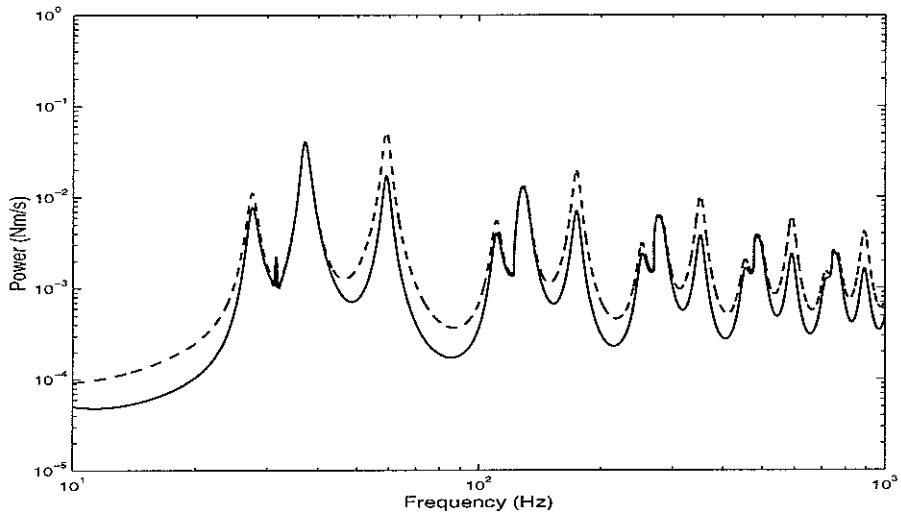

Figure 27. Comparison of power inserted to the built-up structure shown in Figure 19 ($\eta_p = 0.05$ in the plate, $\eta_b = 0.05$ in the beam, point force applied at $x = 0$). ——: power input to the plate (equivalent to dissipated power by the plate), — —: total power input to the built-up structure.

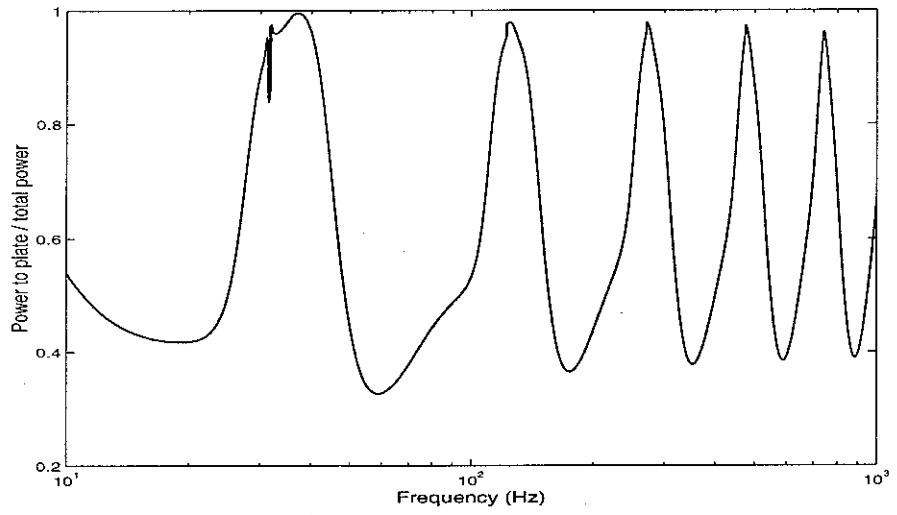

Figure 28. Ratio of the power input to plate to the total input power.

A 3-dimensional diagram can help in understanding the power distribution as a function of frequency as well as the position along the beam. Figure 29 shows the 3-dimensional diagram

showing the power distribution. It should be noted that the power distribution at the position along the beam shows only the input power transmitted to the plate at that specific position x. This differs from the power transmitted to the plate, shown in Figure 27, which is the total power transmitted to the plate. As shown in figure, the power level reduces at high frequency. Note that at both ends $x = 0$ and $x = 2.0$, the power is higher than at other positions. This is because the beam behaves like a free-free beam and therefore near field effects on both ends are generated. At one end of the beam $x = 0$, the power is much higher than that at the other. This is because the force is applied at this point, whereas the level on the beam reduces along its length due to the power transmitted to the plate.

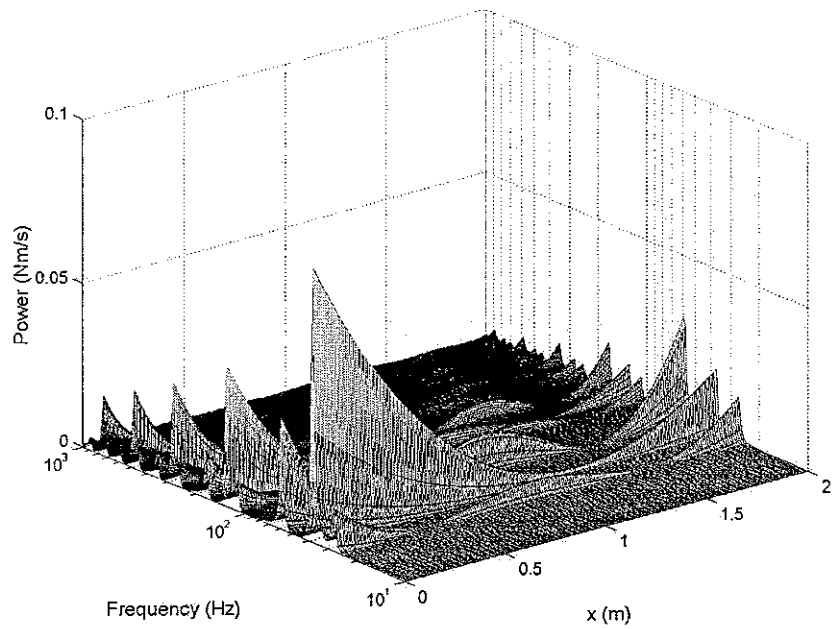

Figure 29. Distribution of vibrational power transmitted to the plate in terms of frequency and the position along the beam

5. Conclusions

The vibrational characteristics of a structure consisting of a beam possessing small wavenumbers and a plate possessing large wavenumbers has been calculated by means of the wave method. The plate is only connected on one side of the beam in the present case, which means that the structure is non-symmetric and thus different from the symmetric structure considered by Grice and Pinnington [11]. The structure was analysed first in terms of an infinite beam and an infinite plate leading to the structure consisting of a finite beam and a finite plate.

Firstly, it was shown that, for the presented non-symmetric structure, the exact line impedance could be simplified so that the plate can be regarded as locally reacting. This means that the line impedance of the plate can be considered as the input point impedance of the corresponding beam of infinite length and unit width driven by a point force, because the wave radiated into the plate has an almost normal direction to the axis of the spine beam. The simplification is based on the assumption that $k_x / k_p < 0.5$, which is verified for the case considered in the present report for the frequency range considered.

Also, it was shown that the coupled wavenumber in an undamped beam is complex because the plate line impedance is complex. This means that the plate behaves like added damping as well as mass when coupled to the beam. The ratio of the imaginary part to the real part of the coupled wavenumber shows that the equivalent loss factor falls with increasing frequency, which was shown by Heckl [13].

The blocking effect was explained. When the finite plate has an anti-resonance, the equivalent loss factor of the beam is maximum and also the mobility level of the built-up structure is minimized. This is because the plate reduces the motion of the beam at this frequency. From this

point of view, it can be said that the flexible finite plate attached to the spine beam behaves like a narrow band vibration damper.

The results of the numerical analysis for a built-up structure consisting of a finite beam and a finite plate were compared to the results of finite element analysis. Below 100 Hz, they agree closely, but above 100 Hz, the resonance frequencies show differences. The main reason is due to the assumption that the neutral axis of the beam lies in the mid-plane of the plate. In reality, it seems to change with frequency. It was verified using a different finite element model in which the neutral axis lies at the centre of the beam for which good agreement was found with the analytical model.

The total input power injected to the structure consisting of a finite beam and a finite plate was compared with the power transferred to the plate. The power transferred to the plate was obtained from the locally reacting impedance of the plate and the velocity driving the plate, which behaves like separate strips. The input power is maximized when there are resonances in the built-up structure. From the ratio of the power transferred to the plate, or power dissipated by the plate, to the total input power, it was seen that the greatest proportion of power is transferred to the plate at specific frequencies which coincide with the anti-resonance frequencies of the plate. This is also explained as the blocking effect.

It should be noted that the results mentioned above are based on some assumptions. Firstly, coupled wavenumbers are calculated based on wavenumber trace matching which is satisfied only when structures have no damping. For application of the wavenumber trace matching in damped structures, it is assumed that the loss factor of the spine is very small and the spine wavenumber is smaller than the receiver wavenumber. Secondly, in the present report, the impedance of the plate is considered as locally reacting. This is satisfied only when the free plate wavenumber is twice as large as the coupled spine wavenumber. Concerning the near field wave

in the coupled beam, it is assumed to have the same value as the propagating wavenumber because only the propagating wave in the coupled beam is obtained from the wavenumber trace matching.

It seems that the wave approach is an appropriate method to analyse the dynamic characteristics of the simple structure. As mentioned in the introduction, the present report will be the first step to approach the development of a practical hybrid method. By means of the wave method, the fundamental dynamic characteristics of a simple combined stucture could be understood.

Concerning further study, it is believed that the present report will be a good basis. In the further study, more complicated structures, such as a structure consisting of four beams and a plate, can be considered. Basically, the approach presented in this report may be used and different methods also can be considered to make progress for mid-frequency analysis.

References

1. O. C. Zienkiewicz and R. L. Taylor 1989 *The Finite Element Method: Basic Concepts and Linear Applications*. London: McGraw Hill; 3rd edition.

2. F. J. Fahy 1994 *Philosophical Transactions of the Royal Society of London* A346 431-447. Statistical energy analysis: a critical overview.

3. R. H. Lyon and R. G. Dejong 1995 *Theory and Application of Statistical Energy Analysis*. Boston: Butterworth-Heinemann.

4. ESDU 97033. Methods for analysis of the dynamic response of structures.

5. ESDU 99009. An introduction to statistical energy analysis.

6. J. C. Wohlever and R. J. Bernhard 1992 *Journal of Sound and Vibration* **153**, 1-19. Mechanical energy flow models of rods and beams.

7. O. M. Bouthier and R. J. Bernhard 1995 *Journal of Sound and Vibration* **182**, 129-147. Simple models of energy flow in vibrating membranes.

8. K. Shankar and A. J. Keane 1995 *Journal of Sound and Vibration*, **185**, 867-890. Energy flow predictions in a structure of rigidly joined beams using receptance theory.

9. K. Shankar and A. J. Keane 1997 *Journal of Sound and Vibration*, **201**, 491-513. Vibrational energy flow analysis using a substructure approach: The application of receptance theory to FEA and SEA.

10. C. T. Hugin 1997 *Journal of Sound and Vibration* **203**, 563-580. A physical description of the response of coupled beams.

11. R. M. Grice and R. J. Pinnington 1999 *Journal of Sound and Vibration* **230**, 825-849. A method for the vibrational analysis of built-up structures, part 1: Introduction and analytical analysis of the plate-stiffened beam.

12. R. M. Grice and R. J. Pinnington 1999 *Journal of Sound and Vibration* **230**, 851-875. A method for the vibrational analysis of built-up structures, part 2: Analysis of the plate-stiffened beam using a combination of finite element analysis and analytical impedances.

13. M. Heckl 1961 *Journal of the Acoustical Society of America* **33**, 640-651. Wave propagation on beam-plate systems.

14. C. Soize 1993 *Journal of the Acoustical Society of America* **94**, 849-865. A model and numerical method in the medium frequency range for vibroacoustic predictions using the theory of structural fuzzy.

15. M. Strasberg and D. Feit 1996 *Journal of the Acoustical Society of America* **99**, 335-344. Vibration damping of large structures induced by attached small resonant structures

16. R. S. Langley and P. Bremner 1999 *Journal of Acoustical Society of America*, **105**, 1657-1671. A hybrid method for the vibration analysis of complex structural-acoustic systems.

17. L. Cremer, M. Heckl and E. E. Ungar 1988 *Structure-borne Sound*. Berlin: Springer Verlag; 2nd edition.

18. D. J. Thompson 2001 *"MSc Lecture notes on Noise and Vibration Control"*, ISVR, Southampton

19. D. J. Thompson 2002 *"ISVR Short Course Lecture notes on High Frequency Modelling of Structural Vibration"*, ISVR, Southampton